U.S. DEPARTMENT OF THE INTERIOR
U.S. GEOLOGICAL SURVEY

STRUCTURAL TRANSECT ACROSS THE NORTH-CENTRAL CARLIN TREND, EUREKA COUNTY, NEVADA

by

Stephen G. Peters[1]

Open-File Report 97-83

1997

[1]U.S. Geological Survey, Reno Field Office, Mackay School of Mines, MS-176, University of Nevada, Reno, Nevada 89557-0047

CONTENTS

List of figures

List of plates

Appendices

Abstract

Gold deposits in the Carlin trend, northern Nev., are aligned along a northwest-trending belt, but definitive geologic parameters have not been documented to account for this alignment. Previous workers in the Carlin trend have documented fold axes in the region, which plunge at low angles to the NE and SW. In addition, many of the folds near gold deposits plunge at shallow angles to the NW or SE. The upper central Betze orebody lies in the north-central part of the Carlin trend in the Goldstrike Mine and is part of the Betze-Post deposits. The orebody is elongated WNW and has a near horizontal plunge, whereas the contiguous and adjacent Post and Deep Post orebodies have NW strikes and SE plunges. The WNW orientation of the upper central Betze orebody appears anomalous, when compared with the strong NW-orientation of the Carlin trend, and with the NW- and SE-plunging fold axes and faults that typify much of the north-central trend. The upper central Betze orebody is hosted in the Dillon deformation zone, which crosscuts the nose of a syncline, parallel to and west of the Post anticline, and generally strikes parallel to the Popovich limestone-granodiorite contact. The orebody is also in the Betze anticline, which may have formed as the result of shear folding along the Dillon deformation zone. A consistent structural grain is present in the WNW-trending upper central Betze orebody. The linear fabric is defined by local WNW-trending fold axes and the planar fabric is defined by a WNW-striking, 20° to 30° NE-dipping zone. The Dillon deformation zone that hosts the upper central Betze orebody is coplanar with all fold axes in the Goldstrike Mine. The Post fault is coplanar with the plunge of the NW-striking fold axes in the Post anticline.

Hydrothermal alteration has significantly affected rocks in and around the orebody, and much of the unique structural disturbance in the orebody may be directly linked with the alteration and mineralization. The upper central Betze orebody is spatially associated with intense decalcification, collapse features, and deformation at the complex contact between the Popovich limestone and Rodeo Creek unit. Several different ore types in the upper central Betze orebody are identified and allow interpretation of the distribution and control of unique oreshoots within the orebody and their geometric and structural relationship to regional structures. At least six separate ore types can be defined, based on geologic setting, mineralogy, geochemistry, and morphology. These six ore types are cataclastic ore, siliceous, sulfidic breccia pods in argillite, disseminated carbonaceous ore, sulfidic breccia pods, arsenic seam ore, and siliceous stibnite-bearing breccia. These ore types are partitioned spatially within the orebody in discrete oreshoots, which have demonstrable spatial relations to the host rock types. The oreshoots are zoned from the footwall to the hangingwall of the orebody with pyrite-rich ores on the top of the orebody, arsenic-rich ores in the central parts, and antimony-rich ores at the bottom.

The Goldstrike Mine also contains the Post anticline, contacts between the Devonian Popovich limestone and Rodeo Creek unit, and the northern contact of the Jurassic Goldstrike stock. The contact zone between Popovich limestone and the Rodeo Creek unit hosts parts of the upper central Betze orebody, and is exposed in the upper parts of the Post anticline. The deformed contact between the Popovich limestone and Rodeo Creek unit, and the several "transitional" facies between the two formations represents the hangingwall part of the upper central Betze orebody. A less-tectonized contact between these two rock units is present in the Post anticline. The contact of the granodiorite with the sedimentary rocks is roughly parallel with the trend of the upper central Betze orebody, and the strike of the Dillon deformation zone. The contact contains numerous apophyses, sills, dikes and irregular-shaped masses of granodiorite away from the main stock. Deformation in the Dillon deformation zone has penetrated into margins of the granodiorite-Popovich limestone contact. Fold axes in the Post anticline also lie at either end of a great circle defining a plane that is parallel to the NW-striking Post fault. The Post fault is most likely coplanar with the plunge of the Post anticline. Fault rocks in current exposures of the fault indicate brittle movement that is in contrast to the ductile folding in the anticline. Either an early ductile Post fault was associated with folding of the anticline and was reactivated later, or the fault post-dated the earlier anticlinal deformation event, and broke along the fabric of the Post anticline.

Introduction

Mine benches in the open pit Goldstrike Mine, north-central Carlin trend (fig. 1), expose the upper central Betze orebody, the Post anticline, contacts between the Devonian Popovich limestone and Rodeo Creek unit, and the northern contact of the Jurassic (Cretaceous?) Goldstrike stock. The Betze orebody is the largest gold orebody in the Carlin trend (Bettles and Lauha, 1991; Leonardson and Rahn, 1996). The orebody has a WNW orientation, with a near-horizontal plunge (Peters, 1996), whereas most of the other orebodies in the north-central part of the Carlin trend are associated with NW-striking faults, such as the Post fault, or NW-striking folds, such as the Post anticline (Volk and others, 1996).

The contact zone between Popovich limestone and the Rodeo Creek unit hosts parts of the upper central Betze orebody, and is exposed in the upper parts of the Post anticline. The Rodeo Creek unit is variable in thickness and lithology throughout most of the Carlin trend; its basal, depositional contact with the Popovich limestone is commonly a bedding parallel fault zone. The upper central Betze orebody parallels parts of the northern contact of the Goldstrike stock. Numerous sill-like apophyses and dikes from the stock and the contact metamorphic aureole are host to parts of the orebody.

This study presents inclined geologic sections through the upper central Betze orebody (pls. 1, 2, 3, 4, 5, and fig. 5), and through the Post anticline (pl. 6), which help to understand the geometry of the upper central Betze orebody, the nature of the Popovich-Rodeo Creek contact in the orebody, and the Post anticline. The sections are derived from approximately 1" = 5' scale mapping of at least 2 to 4, 20– to 40–ft-high mine benches above the 4,800–ft level. The mapping scale has been reduced to approximately 1" = 15' for portrayal on pls. 1-6.

The host rocks in the upper central Betze orebody and the Post anticline are altered and deformed. The accompanying discussion, plates, and figures provide a one–mile-long, detailed structural transect across these rocks in the north-central Carlin trend. Complex structural geology in the Goldstrike Mine has been described by Sampson (1993), Volk and others (1996), and Leonardson and Rahn (1996). Peters (1996) discussed the WNW-striking Dillon deformation zone (DDZ) that hosts the upper central Betze orebody. At least six ore types were identified in the upper central Betze orebody, based on geologic setting, mineralogy, geochemistry, and morphology. The ore types are summarized by Peters (1996) and are partitioned spatially in the orebody in discrete oreshoots.

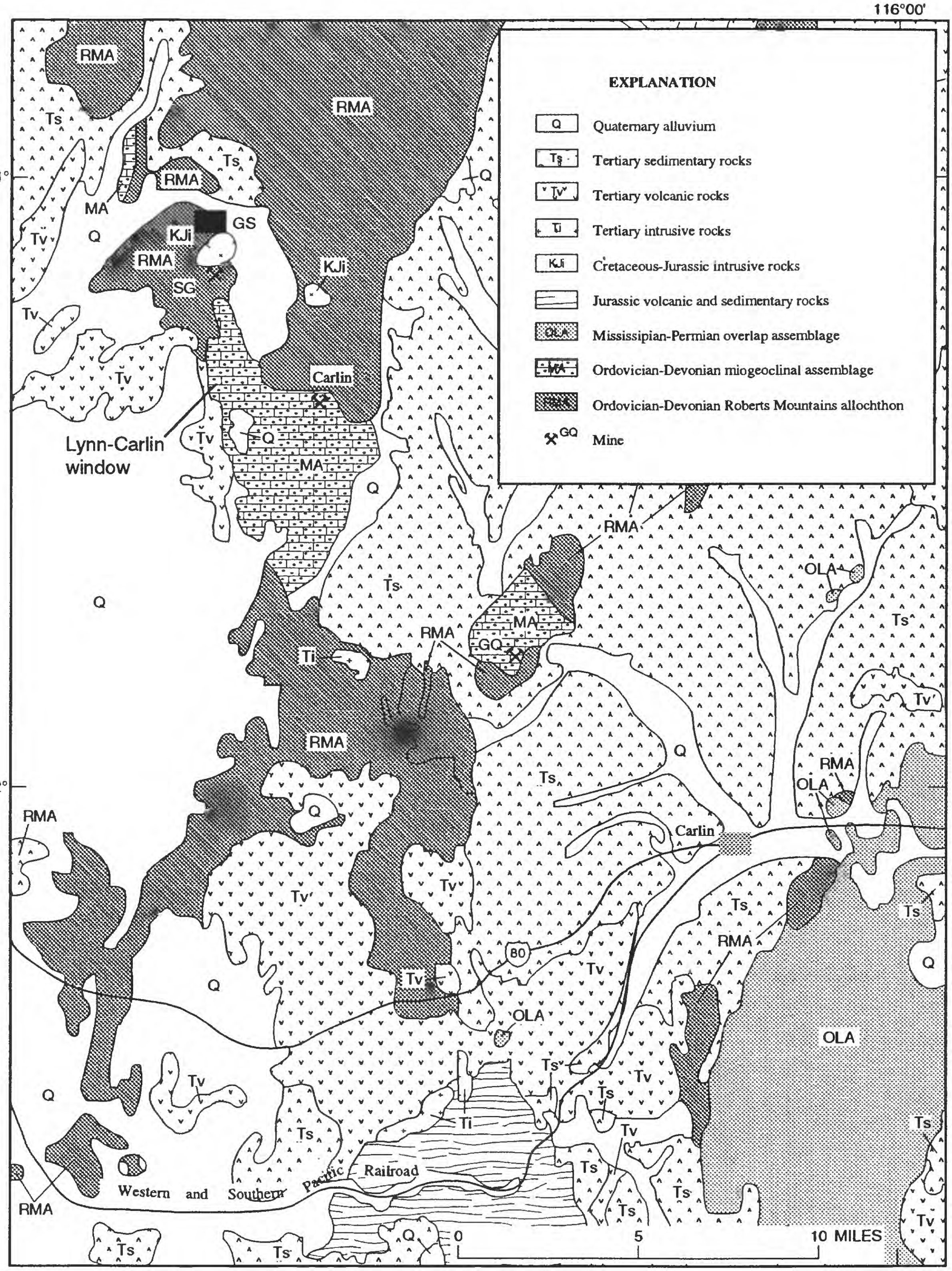

fig. 1. Geology of the Carlin trend area, modified from Stewart and Carlson (1976) and location map. Black rectangle shows location of this study. Most mines are along a NW-trending zone in and around tectonic windows of lower plate rocks (MA), which under lie the Roberts Mountains allochthon (RMA). GQ = Gold Quarry Mine, SG = Genesis-Blue Star mine, GS = Goldstrike Mine, Betze-Post deposits.

Structural data collected from the mine benches is contained in Appendices I-VI, and represents data on plates 1-6 respectively. Fold and structural analyses were performed on most of the bedding attitude data, using the Stereonet V.9.5 program for MAC. In most cases, fold axes were measured or calculated from bedding attitudes in individual mesoscopic-scale folds. Numerous other bedding attitudes were also analyzed in areas where folds were not always apparent, but where deformation was intense. The large data sets of bedding attitudes usually resulted in "beta" (β) fold axes that are coaxial with individual measured folds.

The inclined geologic sections indicate that the upper central Betze orebody is contained in highly deformed rocks. Most inclined geologic sections (pls. 1-5) contain ore-grade material that ranges between 0.02 oz/t Au to as much as several oz/t Au. Barren or lower grade material is present in plate 6, in most of the Post anticline, in the northwestern part of plate 5, and in the western parts of plates 1 and 4, where large masses of granodiorite are present. Descriptions of the various ore types are detailed below.

Geologic Setting

Generally accepted reconstructions of the tectonic history of the region around Carlin, Nev., suggest that early and middle Paleozoic, deep-water sedimentary and igneous rocks were thrust eastward approximately 75 to 200 km during the Late Devonian to Early Mississippian Antler orogeny. These rocks compose the Roberts Mountains allochthon, which lies upon coeval shallow-water rocks of the continental platform (fig. 1). The two packages of rocks, the upper and lower plates, are separated by the Roberts Mountains thrust (Roberts and others, 1958). Emplacement of the allochthon produced a topographic high, which shed sediments, that constitute the overlap assemblage of rocks, to the east and west in the late Paleozoic (Roberts, 1960; Madrid and others, 1992). Other reconstructions of the tectonic history suggest: (1) Early Triassic emplacement of the Roberts Mountains allochthon (Ketner and Alpha, 1992; Ketner and others, 1993); (2) significant tectonism in the region during the late Jurassic Elko orogeny; (3) the Cretaceous to early Tertiary Sevier orogeny; and, (4) large-scale extensional detachment faulting in the late Eocene to early Oligocene (Thorman and others, 1991a, b).

The gold deposits in the Carlin trend are aligned along a NW-trending belt (Roberts, 1960, 1966; Thorman and Christensen, 1991), but definitive geologic parameters have not been shown to account for this alignment. Previous workers in the Carlin trend (Evans and Theodore, 1978) have documented fold axes in the region of the Carlin trend, which plunge at low angles to the NE and SW. This orientation is consistent with orientations documented by Oldow (1984) who noted a relative consistency to deformation symmetry in the Roberts Mountains allochthon and attributed this symmetry to movement and emplacement of the allochthon. However, fold axes in the trend, particularly near mineralized areas, plunge at shallow angles to the NW (Madrid, 1987; Madrid and Bagby, 1986; Volk and Zimmerman, 1991; Peters and Evans, 1995). The NW-trending fold axes were postulated by Evans and Theodore (1978) to be due to Jurassic tectonism, which is compatible with the timing of other tectonic events proposed by Ketner and Smith (1982), Ketner (1987) and Thorman and others (1991b) in northeastern Nevada.

The NW- and SW-trending folds, mostly in the lower plate para-autochthonous miogeoclinal assemblage, are present in the north-central Carlin trend (Peters, 1997a, b). This NW-trending zone also coincides with NW-striking ductile and brittle faults that dip at high angles to the NE, and are coplanar with the fold axes. This study describes outcrop-scale folds, and faults in the Goldstrike Mine, and their structural and geometric relations to these two main fold axis orientations.

Goldstrike Mine Investigations

The upper central Betze orebody lies in the north-central part of the Carlin trend in the Goldstrike Mine (GS on figure 1), and is part of the Betze-Post deposits (Leonardson and Rahn, 1996). The orebody is elongated WNW and has a near-horizontal plunge, whereas the contiguous and adjacent Post and Deep Post orebodies have NW strikes and steeper SE plunges (fig. 2). Orientation of the Post orebodies is similar to the NW-plunging fold axes in the north-central Carlin trend. These orebodies lie adjacent to the Post fault in the NW- SE-plunging Post anticline, and plunge roughly parallel with the multiple fold axes in that fold.

The WNW orientation of the upper central Betze orebody appears anomalous, when compared with the strong NW-orientation of the Carlin trend, and with the NW- and SE-plunging fold axes and faults that typify much of the north-central trend. Analysis of structures in the orebody was undertaken to determine if a structural grain could be defined in the host rocks in and adjacent to the upper central Betze orebody that could account for the consistent, horizontal WNW plunge of the orebody. The accompanying inclined geologic sections, figures, and discussion provide evidence that the upper central Betze orebody lies in a WNW-striking deformation zone (figs. 2 and 3).

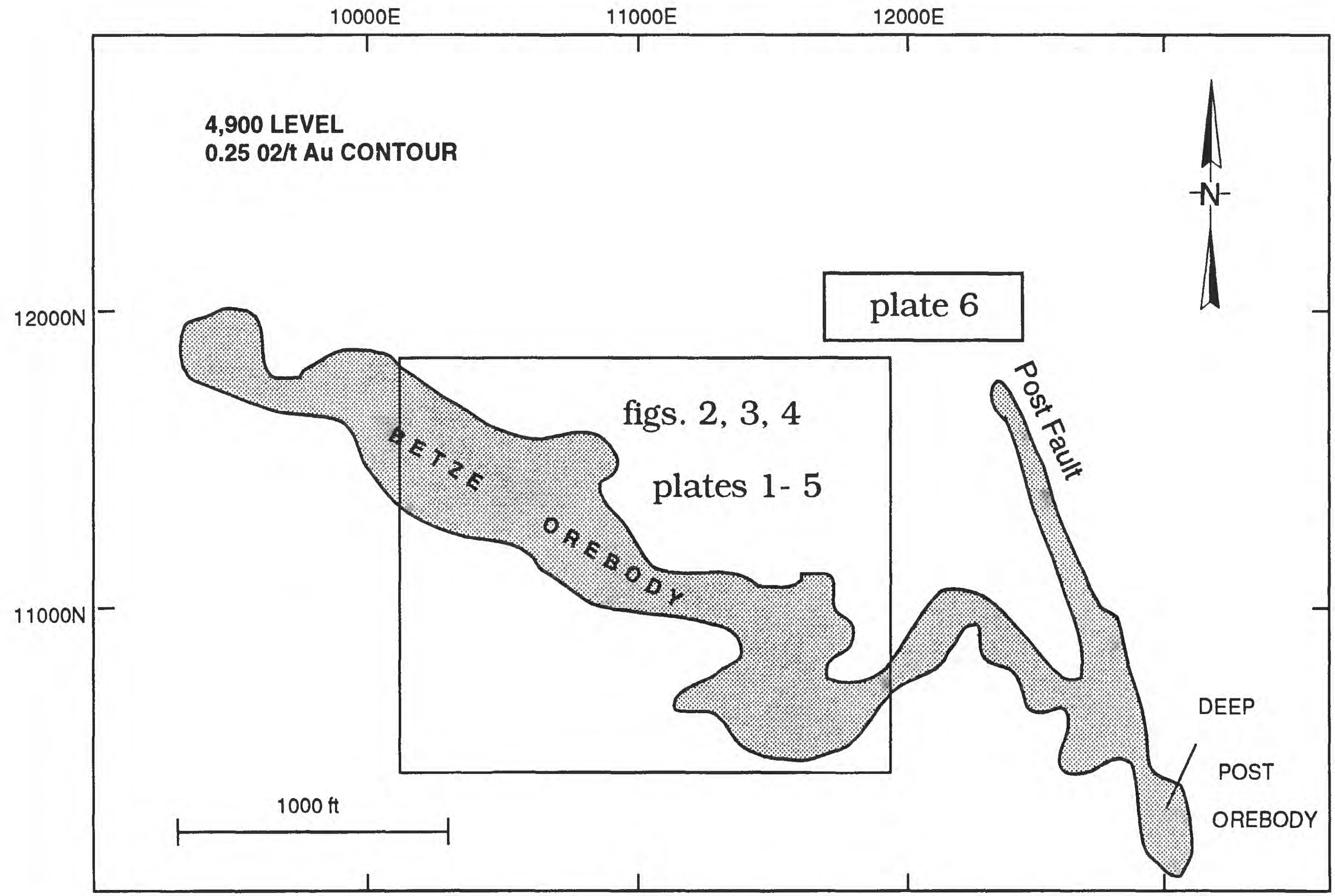

fig. 2. Map of the upper central Betze orebody, 4,900 ft Level, showing the outline of the 0.25 oz/t Au contour, and location of the Deep Post orebody. The Deep Post orebody has a NW strike, parallel to the plunge of the Post anticline and the Post fault. The NW elongation of the Post orebody is roughly coincides with the footwall of the Post fault. Adapted from Peters (1996).

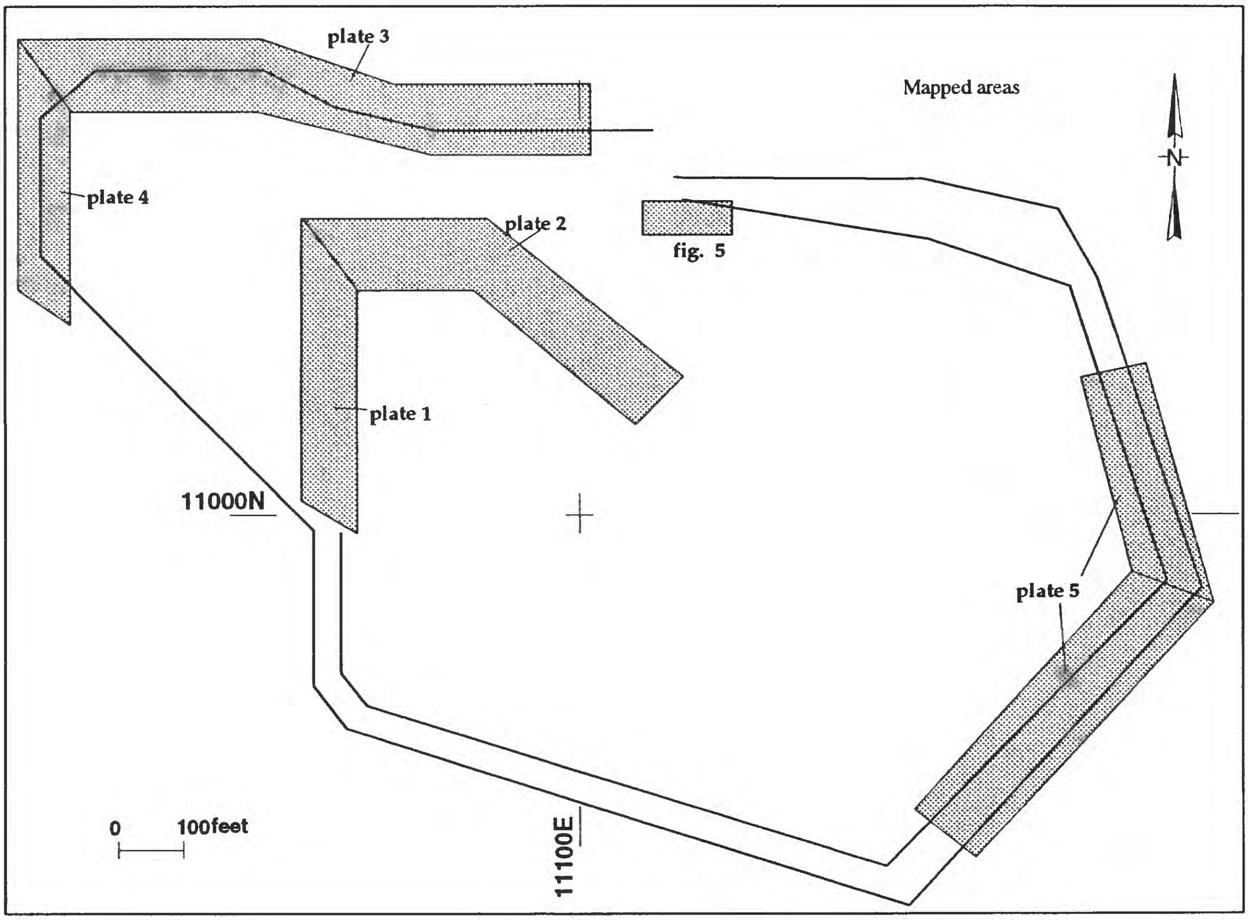

fig. 3. Index map showing locations of inclined geologic sections mapped in the upper central Betze orebody (pls. 1, 2, 3, 4, and 5, and fig. 5). The western and northern mine faces of the upper central Betze orebody were mapped at approximately 1:10 scale (1 cm = 1 m). See fig. 2 for location.

The upper central Betze orebody is hosted in the upper parts of the Devonian Popovich limestone and in the lower parts of the Devonian Rodeo Creek unit, which are both lower plate rocks that are in contact with the northeastern part of the Goldstrike granodiorite stock (Lauha and Bettles, 1993; Arehart and others, 1993; and Smith and Sharon, 1994). The parts of the Rodeo Creek unit that are mineralized are present in the nose of a NW-trending syncline that lies to the west of the Post anticline. Rock types hosting the orebody include black to gray, carbonaceous shale, mudstone, argillite, white to gray limestone, hornfels, granodiorite, and breccia (fig. 4).

Hydrothermal alteration has significantly affected rocks in and around the orebody, and much of the unique structural disturbance in the orebody may be directly linked with the alteration and mineralization. The upper central Betze orebody is spatially associated with intense decalcification, collapse features, and deformation at the complex contact between the Popovich limestone and Rodeo Creek unit (pls. 2 and 3). Significant structures in the envelope of alteration and mineralization of the upper central Betze orebody are the WNW-striking Betze anticline and the Dillon fault zone. Both these structures are interpreted to be related to the same deformation event.

Dillon deformation zone

The Dillon fault zone in the upper central Betze orebody is one of several shear zones that comprise a broad, deformed, 200–m-thick zone—the Dillon deformation zone (DDZ)—that has a footwall near the granodiorite-Popovich limestone contact to the south, and grades upward with various sheared strands into the basal, lithic interval of the Rodeo Creek unit in the core of the NW-striking syncline to the north (fig. 4).

Strain in the DDZ is heterogeneous and was partitioned differently in each package of rocks that it traverses. Deformation intensity and style between sheared strands reflect rock type. Within the zone, undeformed phacoidal clasts, slabs, and blocks occur in sheared pelitic zones, which anastamose around them (pls. 1-4). Several individual, carbonaceous, sheared strands, such as the Dillon fault zone, extend laterally in the DDZ (fig. 4). The carbonaceous Dillon fault zone lies in the footwall of the Popovich limestone-Rodeo Creek unit contact. Southeast of the synclinal hinge, of rocks of the Rodeo Creek unit, the DDZ enters unaltered Popovich limestone, and is focused mainly along one or more central carbonaceous strands (fig. 4; pl. 4). Deformation in the DDZ is most intense along these decalcified, carbonaceous, sheared strands.

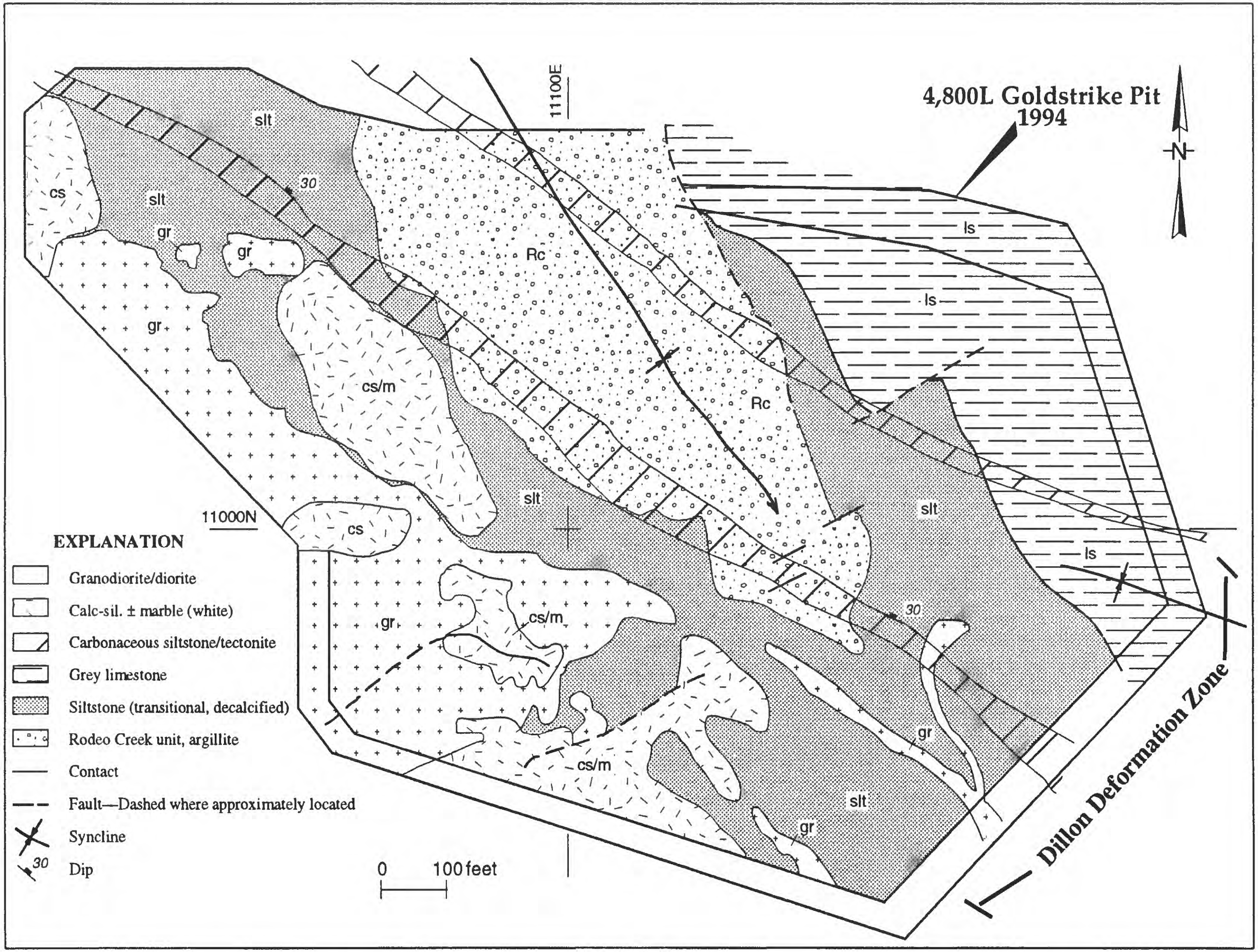

fig. 4. Generalized geologic map of the upper central Betze orebody on the 4,840 ft Level, from 1"=50' scale compilation and from 1"= 200' mapping on floor muck of the open pit by Jerry Rahn, Barrick Goldstrike Mines and adapted from Peters (1996). WNW-oriented hatached zones are individual strands of the DDZ, such as the Dillon fault.

Most fold axes in and immediately adjacent to the upper central Betze orebody plunge at shallow angles to the NW, NNW, or ESE; a few mesoscopic folds also trend NE and E at low angles (Appendixes I-VI). The majority of fold axes lie along a great circle that approximates a plane dipping 27° NE and striking approximately 300°. This plane is parallel to the *Dillon fault*, a 10–m-wide strand of the DDZ, and parallel to the 200–m-wide zone of deformation that hosts the upper central Betze orebody.

The Betze anticline, not shown of figure 4, which is a composite shear fold, is parallel and contained in the DDZ. The shear fold is truncated by the main body of granodiorite on the south (pls. 1-4), but apophyses of the granodiorite in the DDZ are intensely deformed and dismembered. Variably decalcified Popovich limestone forms the footwall to the DDZ in the vicinity of the Betze anticline, where phacoidal-shaped blocks are composed of white, crystalline limestone, surrounded by planar, foliated zones of decalcification and local brecciation (pls. 1, 4, and 5).

In the central part of the upper central Betze orebody (eastern part of pl. 2), black, carbonaceous, decalcified rocks in the Dillon fault zone contain several tight folds with red breccia in their cores. This intensely folded area is directly down plunge and to the north of a similar area portrayed in figure 5. The Dillon fault zone in the upper part of the Popovich limestone, in contact with the lower argillite horizon of the Rodeo Creek unit, shows intricate flow-like folding of white and black, clay-rich siltstone (fig. 5). These folded areas are overlain by a 2– to 5–m-wide zone, which contains a large, gray, sulfidic breccia body, composed of decalcified limestone and siltstone. Above this zone lies a thick, red, brecciated zone of argillite.

The DDZ is coplanar with most the fold axes in the region and is proposed to be the result of late, regional strain (Peters, 1997a, b). The DDZ is interpreted to occupy a recumbent axial plane, which rotated NE-striking fold axes into NW-striking fold axes. Only folds contained directly in the DDZ have fold orientations that are WNW-striking, because the deformation and strain there was highly focused and penetrative.

These WNW-striking shear folds are similar to wrinkles, generated in the plane of the shear zone, and are secondary and subsidiary to the main rotation or shearing of the original NE-striking fold and fault fabrics in the north-central part of the Carlin trend.

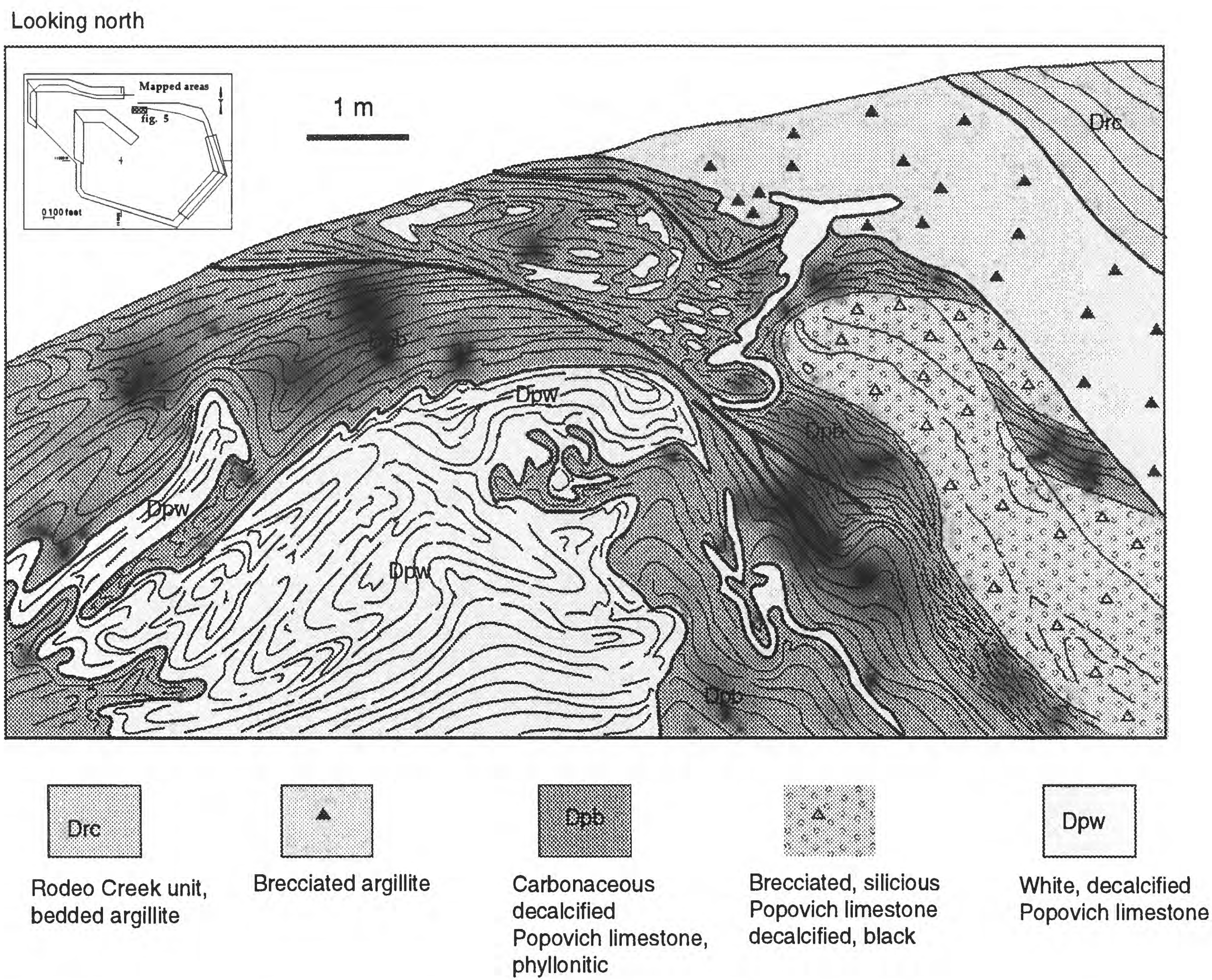

fig. 5. Idealized sketch of a cross section through the central Betze orebody, looking WNW. General zoning in the orebody is Fe (iron) on the top, As (arsenic) in the central parts, and Sb (antimony) at the bottom. See text.

Mesoscopic phacoids of competent, crystalline limestone are surrounded by decalcified, gray seams of deformed limestone (now siltstone), which anastamose around them (pls. 1 and 4). Because this type of deformation is common throughout the DDZ, it is likely that dissolution, transport, fluid flow, plucking, and high strain were processes that were active during the generation of the phacoids and the sheared seams which surround them.

Fabrics in the upper central Betze orebody, as well as the style of deformation outlined above, indicate that strain was accompanied by dissolution. The coincidence of gold and other geochemical enrichments in these zones suggest that deformation, decalcification, and fluid flow could have been linked in time and in space, such that mineralization and deformation along the DDZ were synchronous.

Clay-rich, cataclastic, sulfidic, gold-rich zones and breccia pods are common in the hangingwall of the orebody and the DDZ (pls. 2 and 3), whereas in the footwall unmineralized marble and limestone forms mesoscopic phacoids separated by conjugate and anastamosing, gray, clay seams, which are locally enriched in realgar, orpiment and gold (pls. 1 and 4).

Geometric relations of folds and shear zones in the upper central Betze orebody aid the interpretation of how the orebody formed and may advance the understanding of how the gold deposits are related to deformation styles in and near the tectonic windows. Folds and faults in the orebody in the north-central Carlin trend, are evidence of events that took place during the tectonic evolution of the region. A generalized three-phase (D_1–D_3) sequence of tectonic events for the Carlin trend area (see Peters, 1997a, b), between the Paleozoic to late Mesozoic, involves: (1) Antler–Humboldt deformation (D_1, F_1 folds) between late Devonian to late Pennsylvanian in age, roughly synchronous with the emplacement of the Roberts Mountains allochthon; (2) Sonoma–Elko deformation (D_2, F_2 folds) between late Permian and late Jurassic in age, noted for abundant and penetrative NE- and SW-trending, shallow-plunging folds, local intrusives, and NW-trending faults; and (3) Sevier deformation (D_3, F_3 folds) between late Jurassic and early Eocene in age, which rotated or refolded many F_2 folds to N- and NW-trends and produced local WNW-trending F_3 shear folds, such as the Dillon deformation zone.

Ore styles

Distribution of gold minerals and alteration in the upper central Betze orebody is related to structure, stratigraphy, and location in the orebody. On the basis of morphology and mineralogy, several different ore types are recognized.

These ore types are spatially separated and crudely zoned, with a tendency for certain types to be in the hangingwall, whereas other types are concentrated in the footwall. Many ore types cluster into elongate internal oreshoots, composed of unique or composite-ore types, and are separated from other oreshoots by waste or low-grade rocks. Separate ore control of many oreshoots directly relates to individual strands of the DDZ.

Mineralogically and geochemically distinct ore types have been noted in Carlin-type deposits by Radtke (1985) and Kuehn (1989). The spatial relations between these ore types have not been well understood, although temporal relations have been suggested (Kuehn and Rose, 1992, 1995; Campbell, 1994; Lamb, 1995). Most workers agree that deposition of pyrite with gold-rich arsenical rims was followed by orpiment-realgar, barite, stibnite and mercury ores. Distinct ore types in the upper central Betze orebody are recognized from the results of this study (fig. 6) and are defined based on geologic setting, mineralogy, geochemistry, and morphology. These ore types are cataclastic ore, siliceous, sulfidic breccia pods in argillite, disseminated carbonaceous ore, sulfidic breccia pods, arsenic seam ore, and siliceous stibnite-bearing breccia. Characteristics of these ore types are designated by letter on figure 5 from hangingwall to footwall of the orebody as follows:

(a) Cataclastic ore is composed of brecciated, decalcified, and locally silicified rocks of the transitional sequence between the Popovich limestone and Rodeo Creek unit, either decalcified limestone or deformed, crushed argillite (pl. 1). These ore zones may be up to 20 m thick, and are usually yellow to creamy tan in color, but may range to dark gray. The zones are commonly surrounded by seams of sheared, carbonaceous rocks. Locally these rocks contain finely layered pyrite and/or marcasite. Blast hole assays show that selected pods grade >0.25 oz/t Au.

(b) Siliceous, sulfidic breccia pods in argillite consist of tectonic breccia, fossil hash, or sedimentary breccias that contain about 0.25 oz/t Au. The pods are 2 to 5 m thick, red, knobby, and up to 20 m long, but may have dimensions of <1 m. The rocks are highly silicified, and locally contain high-pyrite contents. They are commonly surrounded, particularly on the hangingwall of the orebody, by carbonaceous or sulfidic, gray to black, deformed clay seams (pls. 1, 3 and 4). Collapse features are also present in about 1 m of the hangingwall of the bodies. This ore type contains elevated values of mercury, thallium, arsenic, nickel, cobalt, and copper. Detrital minerals in the transitional sequence rocks contribute high values of uranium, rare earths and titanium. Not all of these breccia pods are mineralized.

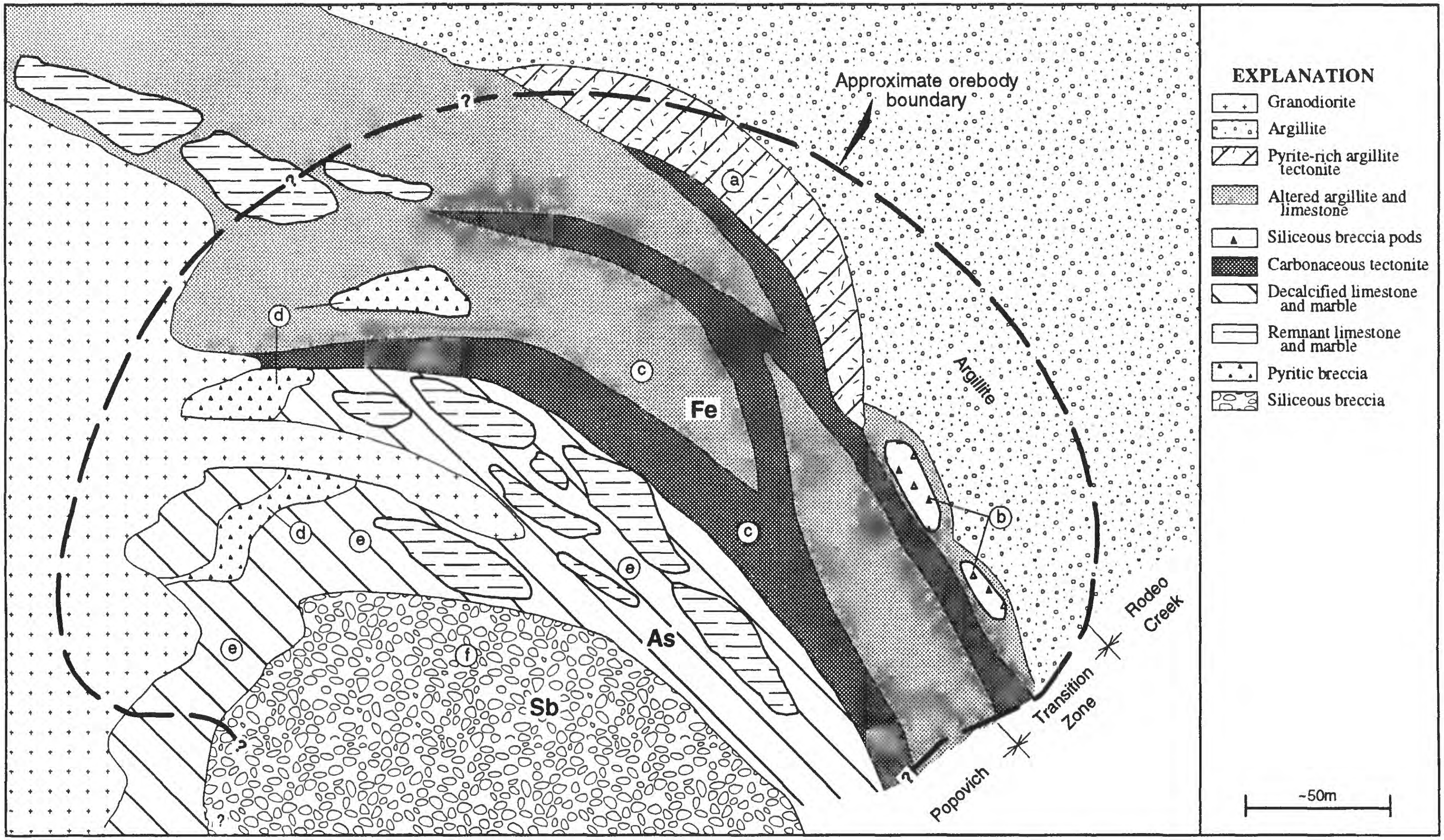

fig. 6. Idealized sketch of a cross section through the central Betze orebody, looking WNW. General zoning in the orebody is Fe (iron) on the top, As (arsenic) in the central parts, and Sb (antimony) at the bottom. The ore types are designated by letter as (a) cataclastic ore, (b) siliceous sulfidic breccia pods in argillite, (c) disseminated carbonaceous ore, (d) sulfidic breccia pods, (e) arsenic seam ore, and (f) siliceous stibnite-bearing breccia.

(c) Disseminated carbonaceous ore is present in shear zones, composed of carbonaceous siltstone, gray breccia and decalcified limestone with local quartz veinlets and marcasite blebs and typically contains 0.10 to 0.250 oz/t Au (pls. 1, 4 and 5). This ore type is also present in undeformed, decalcified rocks as disseminated pyrite replacements. Gold is associated with 1 to 10 micron-size arsenic- and thallium-rich rims on pyrite. The most common ore is gray to olive-gray, or locally hematite-red in color. Gold distribution in these zones is not uniform. Geochemically this ore type has high values of mercury, chromium, zinc, and copper.

(d) Sulfidic breccia pods are irregularly shaped, siliceous ore pods, usually located adjacent to the granodiorite-limestone (marble) contact in the footwall of the DDZ (fig. 6). The pods are as large as 10 X 30 m (pls. 1-4). Location of these ore pods is partially localized by steeply-dipping, NW-striking, narrow, phyllonitic faults, which crosscut the relatively shallow-dipping stratigraphic units. The pods are black to dark gray, are relatively hard and locally contain clay, decalcified limestone, and silica hornfels fragments. This ore type has high-gold (>0.50 oz/t Au) and high-sulfide content; realgar, orpiment and stibnite are generally lacking. Geochemically, the ore is rich in barium, copper, mercury, and zinc, and moderately rich in arsenic.

(e) Arsenic seam ore is predominantly realgar-orpiment-rich, but is also pyrite- or marcasite-rich. This ore is typically composed of decalcified seams of sheared limestone and calc-silicate rocks containing barren phacoids of crystalline, white limestone and marble (fig. 6). Some seams zone laterally into sulfidic breccia bodies, similar to those found in ore types *c* or *d*. The seams on either side of many apophyses and phacoids of granodiorite contain orpiment-realgar and gold (pl. 5). The contact zones between the seams and the granodiorite, are 10 cm thick, white to gray, and contain sucrosic quartz hornfels. The altered gray clay seams next to these apophysy contacts are derived from granodiorite and from inclusions of gray siltstone (decalcified limestone) on the margins of the apophysy. Vertical joints in the granodiorite and adjacent siltstone contain realgar-orpiment and mark the fluid pathways between seams. This ore type is best developed in seams of decalcified limestone that surround phacoids of unmineralized marble and limestone. In the southeastern upper central Betze orebody, this type of seam ore grades about 1 oz/t Au, and the barren limestone phacoids form at least 40% to 60% of the mass suggesting that the realgar-orpiment seams carry greater than 2 oz/t Au (figs. 7a, b, and c). Geochemically, this ore type is dominated by arsenic.

(f) Siliceous stibnite-bearing breccia is present in the footwall of the other ore types described above in an arcuate, homogeneous, hard, dark-gray, siliceous breccia zone (pl. 4). Stibnite is present as fracture coatings and vug fillings along with calcite and barite, and forms veinlets, and occupies both clasts and matrices in dense silica. Marcasite veinlets crosscut and most likely postdate the silica stibnite stage. Geochemically, the ore is rich in antimony and moderately rich in mercury, thallium, arsenic, barium, and zinc.

Zoning and control of internal oreshoots

The main geologic features in the upper central Betze orebody are: (1) the syncline developed in the Rodeo Creek unit (argillite) in the central part of the orebody; (2) transitional rocks and decalcified rocks of the Popovich limestone, surrounding this syncline; (3) marble, calc-silicate rocks and limestone, and, (4) granodiorite (fig. 4). Two major, WNW-striking, carbonaceous strands of the Dillon deformation zone traverse the eastern and western limbs of the syncline that lie west of the Post anticline.

Oreshoots in the upper central Betze orebody are hosted in argillite, sulfidic breccia, shear seams and the Dillon fault strands. Contours of gold content in the orebody (fig. 7a) indicate that these oreshoots are concentrated along the WNW-trending granodiorite-transitional rock contact zone, the NW-striking Dillon fault zones and in east-west zones lateral to the Dillon fault and east of the granodiorite contact (fig 7a). The east-west zones of high gold values define oreshoots that coincide with EW-striking, N-dipping faults and the WNW-trending folds.

Distribution of sulfur in the upper central Betze orebody reveals WNW-striking trends that are parallel to the granodiorite-Popovich limestone contact. These zones coincide with many of the sulfidic breccia ore pods and a large oreshoot of high arsenic seam ore to the SSE (fig. 7b). These breccia and seam oreshoots are parallel to and lie in the footwall of the Dillon fault (fig. 7a). A smaller pod of highly sulfidic ore lies in a carbonaceous shear zone in argillite in the hangingwall of the Dillon deformation zone.

Several areas of carbonate in the upper central Betze orebody contain >10% carbonate (fig. 7c). The area in the northeastern part of figure 7c coincides with gray, unaltered, relatively undeformed limestone of the Popovich limestone on the western edge of the Post anticline. The northwestern areas of >10% carbonate coincide with calc-silicate rocks and marble at the granodiorite-Popovich limestone contact. High-grade marcasite-pyrite, siliceous breccias carrying high gold grades occur at the margins of the low-grade or barren high-carbonate zones. The processes of ore formation in these oreshoots involved decalcification of the limestone, marble, and calc-silicate rocks. The southeastern >10% carbonate zone represents a high-grade realgar-orpiment seam ore; the high-carbonate content results from the barren, resistant phacoids present in the oreshoot.

Popovich limestone-Rodeo Creek unit contact

The deformed contact between the Popovich limestone and Rodeo Creek unit, and the several "transitional" facies between the two formations, are portrayed on plates 2 and 3, and fig. 5. This contact represents the hangingwall part of the upper central Betze orebody. A less-tectonized contact between these two rock units is present in the Post anticline (fig. 2; pl. 6).

Faults and folds present in the transitional rocks of the Popovich limestone-Rodeo Creek unit contact are complex (pls. 1-5; figs. 8 and 9; Appendixes I-V). In the western part of plate 2, white crystalline marble is decalcified and deformed by seams of gray and black clay, the main strand of the Dillon fault zone. Argillite of the Rodeo Creek unit forms the hangingwall of the transitional zone, and also locally lies in lobes that are surrounded by altered Popovich limestone rocks composed of siltstone, deformed clays and decalcified limestones (pl. 1). Hangingwall strands of the DDZ cut bedding acutely in the argillite of the Rodeo Creek unit and transitional rocks, above the Popovich limestone-Rodeo Creek unit contact.

Parts of the contact between the Popovich limestone and the Rodeo Creek unit show evidence of a separate tectonic event, prior to movement on the Dillon deformation zone. Hangingwall to the main carbonaceous strand of Dillon fault zone lie a transitional zone of sandstone, brown, slatey, phyllonitic mudstone, and red, knobby breccia bodies (pls. 1 and 3). Many of these rocks contain tectonic fabrics, which have been dismembered into phacoidal slabs and blocks by the Dillon Deformation zone. The older tectonized zone is overlain by a white, brecciated, locally sulfidic, cataclasite body, which consists of a mixture of deformed argillite and decalcified, transitional limestone, and mudstone (pls. 2 and 3). The remnant blocks and slabs that contain tectonized fabrics in the Popovich limestone-Rodeo Creek contact zone suggest that an older deformation event took place along the contact, but has been overprinted by shearing and folding in the Dillon deformation zone.

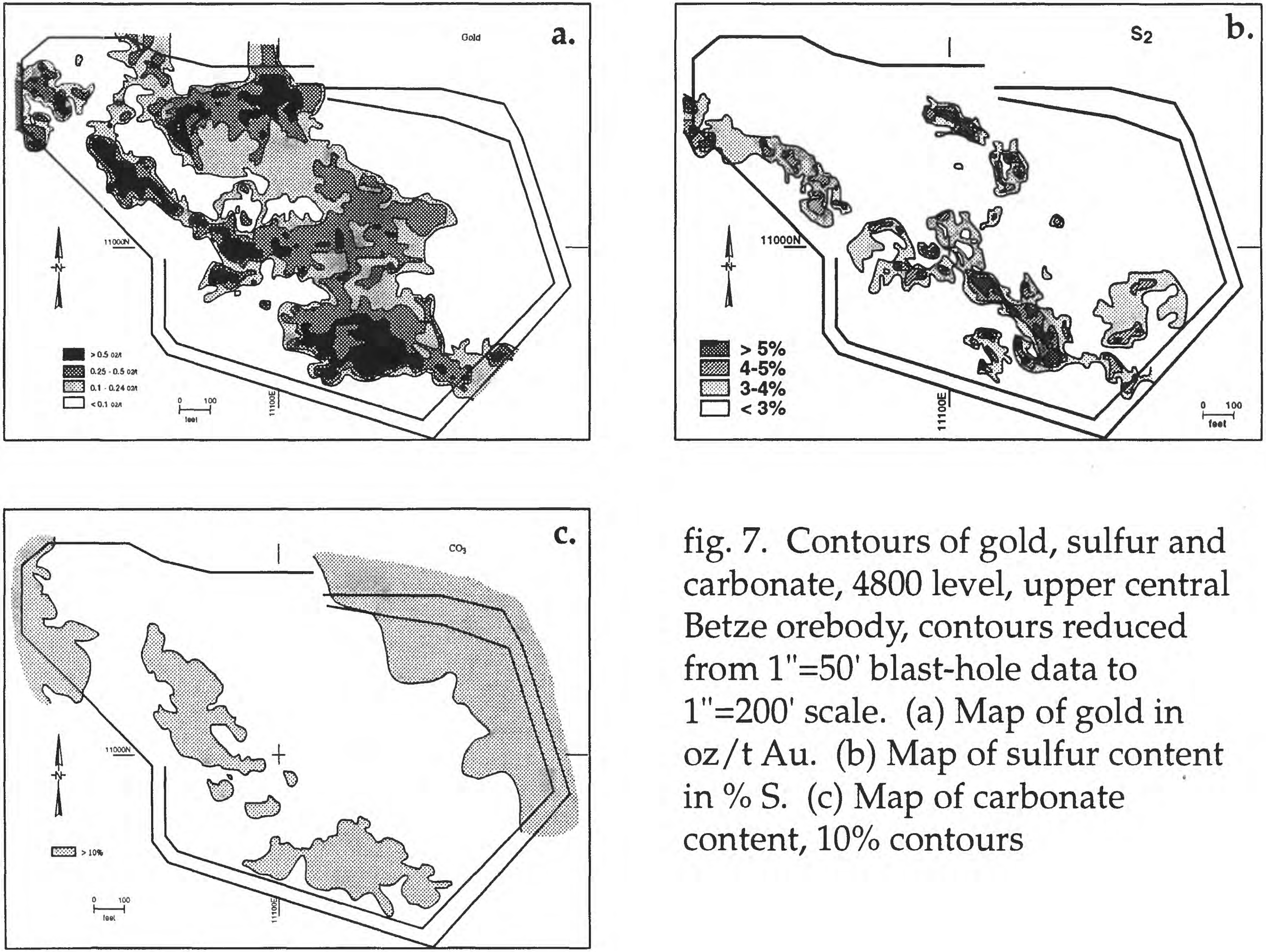

fig. 7. Contours of gold, sulfur and carbonate, 4800 level, upper central Betze orebody, contours reduced from 1"=50' blast-hole data to 1"=200' scale. (a) Map of gold in oz/t Au. (b) Map of sulfur content in % S. (c) Map of carbonate content, 10% contours

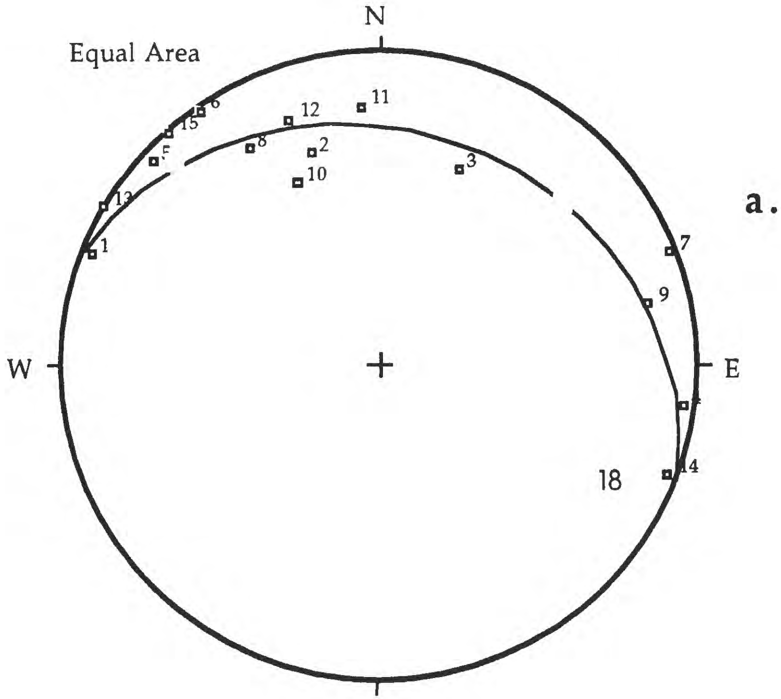

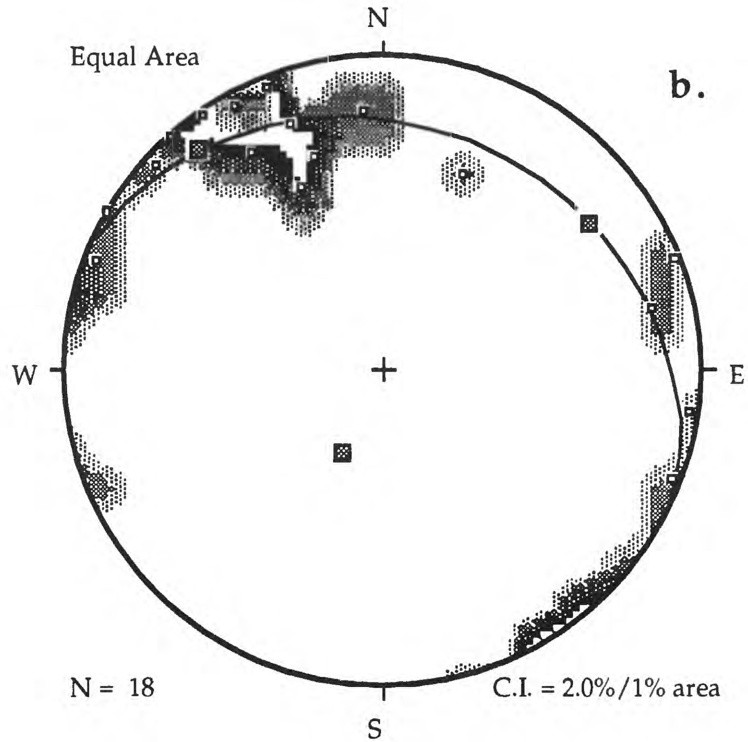

fig. 8. Stereographic net plots, upper central Betze orebody.
(a) Equal area plot of fold axes from pl. 2 (Appendix II) and computer best-fit plane to those fold axes, which approximates the Dillon deformation zone. Fold axes that strike WNW and ESE are shear folds in the Dillon deformation zone. Fold axes that plunge to the NW and NE are older folds, such as the Post anticline.
(b) Similar plot to 7a, but with the addition of three WNW-striking fold axes from pl. 1, with a 1% contour and a best fit plane that also approximates the Dillon deformation zone. Boxes keyed to numbers:

Total Fold axes
calculated by stereographic net
North face 1-15

1. 291 4 Footwall rocks, without folds
2. 342 30 Total argillite rocks, w/ folds, Drc
3. 22 34 Central argillite w/o folds, Drc
4. 98 4 Total footwall (Dillon fault) zone
5. 312 4 "CBC" zone, hangingwall area
6. 325 2 Top (hangingwall) argillite, Drc
7. 69 2 Hangingwall to Dillon fault (Dpg, Dpw, Dpb)
8. 329 21 North Face total bedding attitudes
9. 77 14 Fold A central argillite (Drc)
10. 336 37 Fold B central argillite (Drc)
11. 356 19 Fold C central argillite (Drc)
12. 240 18 Fold D central argillite (Drc)
13. 300 0 Fold E central argillite (Drc)
14. 111 3 Fold F central argillite (Drc)
15. 318 1 Fold G central argillite (Drc)

Best fit plane to fold axes is 201/64 ~ Dillon fault zone

Red, silicified breccia bodies, with high gold contents, are common along the Popovich limestone-Rodeo Creek unit contact (pls. 2 and 3). These breccia bodies are quasi-stratigraphic and some are locally folded around the nose of a tight, recumbent, isoclinal fold. These breccia bodies lie close to the older tectonized zone described above (see pls. 2 and 3). The red, siliceous breccia bodies are of three types: fossil hashes; fault breccias; and sedimentary breccias. In the extreme east of figure 5, red moderately undeformed argillite lies upon the red breccia body. This area represents the northern limb of the south part of the pointed keel of the NW-trending syncline of the Rodeo Creek unit, which is crosscut by the Dillon deformation zone (fig. 4). Some of these red breccia bodies may indicate a pre-DDZ shallow-dipping shear zone at the Popovich limestone-Rodeo Creek unit contact.

The contact between the Popovich limestone and Rodeo Creek unit at the top of the Post anticline is, by contrast, relatively concordant, although the rocks along the contact and in the anticline are deformed (pl. 6). The Post anticline and syncline to the west form cuspate shapes between the Rodeo Creek unit and Popovich limestone, with the pointed terminations pointing downward into the more competent Popovich limestone (Peters, 1996). In the upper parts of the synclinal fold, and at the top of the Post anticline, the fold shape is round. In the crowded, downward-pointed termination of the syncline, however, the rocks are highly deformed and the fold is V-shaped. The deformation in this synclinal hinge was enhanced in the area of the upper central Betze orebody by the heterogeneity of the transitional rocks at the contact between the Popovich limestone and the Rodeo Creek unit. Additional factors that may have enhanced deformation and were related to mineralization are widespread dissolution, shearing, decalcification, fluid flow, and folding.

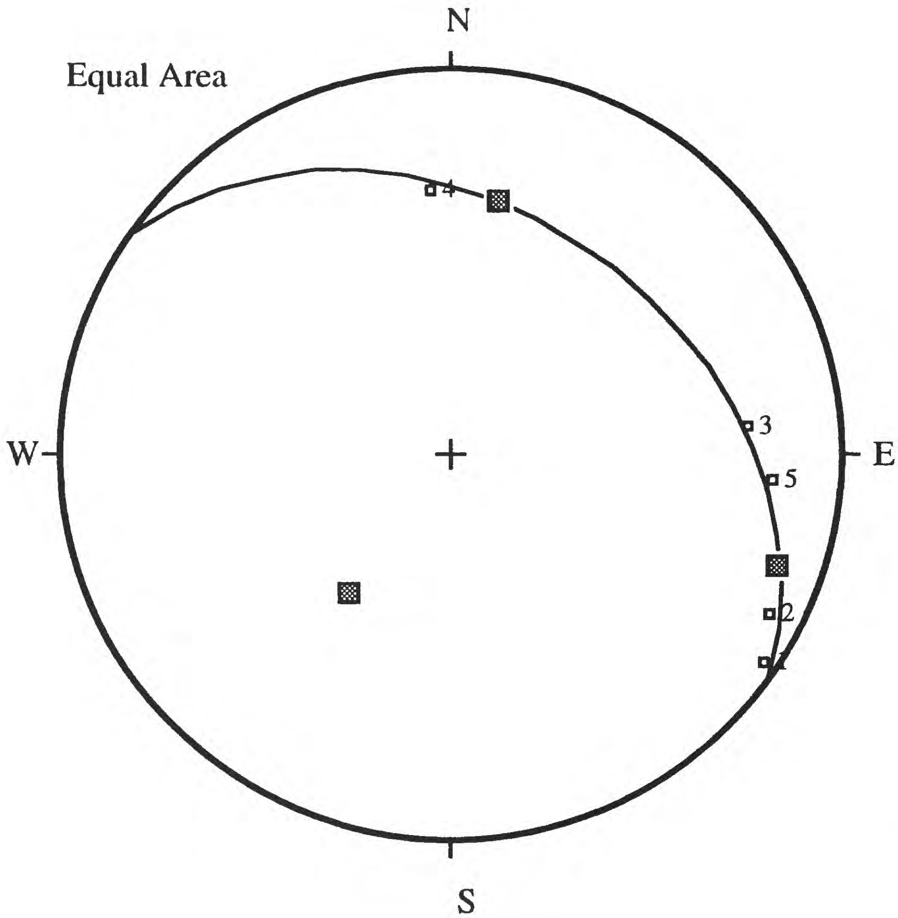

fig. 9. Stereographic net plot, upper central Betze orebody showing fold axes from plate 4, and the west part of plate 5, with a best fit plane that also approximates the attitude of the Dillon deformation zone (Appendexes IV and V). The fold axes plotted here and on figure 7 indicate that well-ordered symmetry is present in the upper central Betze orebody, and that a symmetry is related to Dillon deformation zone. Numbers keyed to boxes:

box	**strike**	**plunge**	**location**
1.	124	3	4,800 Level North Face ls
2.	117	9	4,880 Level West Face
3.	85	24	4,800 Level West Face
4.	356	32	4,840 Level West Face
5.	95	18	Total bedding West Face w/o N Face ls

Contact of the Goldstrike stock

The contact of the granodiorite with the sedimentary rocks is roughly parallel with the trend of the upper central Betze orebody, and the strike of the Dillon deformation zone. The contact contains numerous apophyses, most of which are sill-like and near-horizontal. Dike and irregular-shaped masses of granodiorite are also present away from the main stock. Fold axes and textures in the upper central Betze orebody (figs. 8 and 9; Appendixes I-V), suggest that deformation in the Dillon deformation zone has penetrated into margins of the granodiorite-Popovich limestone contact.

Phacoids of granodiorite, limestone and marble are developed where apophyses are deformed in the central, sheared strands of the DDZ (pls. 1, 4 and 5). Examples of this deformation style are most common in the footwall parts of the Dillon fault zone, where partially decalcified limestones and apophyses of granodiorite form phacoids, and are surrounded by seams that anastamose around the phacoids (pl. 5).

Several large, siliceous, pyritic breccia bodies are present near the granodiorite contact (pls. 1, 4 and 5; fig. 6), which are distinct from the red, siliceous breccia bodies at the Popovich limestone-Rodeo Creek unit contact (pls. 2 and 3). These siliceous pyrite breccia bodies form high-grade oreshoots, along the southwestern margin of the central Betze orebody along the granodiorite contact.

The dismembered and deformed granodiorite and calc-silicate rocks indicate that some deformation along the northern contact of the Goldstrike stock was post-Jurassic (Cretaceous?) in age. The spatial association of the high-grade pyritic breccia zones with the contact suggest that the contact zone had geochemical and physical properties that were not present in other parts of the Dillon deformation zone, and the upper central Betze orebody.

Post anticline

The crest of the Post anticline is portrayed on plate 6 on a 1993 wall of the Goldstrike Mine (figs. 2 and 10). Additional bedding attitudes were collected beneath this area in 1996 (fig. 10; Appendix VI). The central core of the anticline is composed of black to dark gray, carbonaceous, locally decalcified Popovich limestone. The overlying Rodeo Creek unit contains a 60–m-thick transitional zone, composed of decalcified, limy shales, and argillite. Breccia bodies in the transitional zone are siliceous, but most appear to be sedimentary rip-up breccias. NW-striking, W-dipping faults, such as the Grand Jean fault (plate 6), are dominant on the west flanks of the Post anticline. The NE-dipping Post fault, on the east side of the anticline, is a brittle structure, in contrast to the ductile folding in the anticline, and in parts of the DDZ to the west. Mesoscopic fold axes in the Post anticline consistently plunge at very low angles to the NW and SE (fig. 11; Appendix VI).

Fold axes in the Post anticline also lie at either end of a great circle defining a plane that is parallel to the NW-striking Post fault (fig. 11). If the Post fault is coplanar with the plunge of the Post anticline, but the fault is brittle in contrast to the folding in the anticline, the fault may have broken in a stress regime different from the deformation that formed the anticline. Either an early ductile Post fault was associated with folding of the anticline and was reactivated later, or the fault post-dated the earlier anticlinal deformation event, and broke along the fabric of the Post anticline.

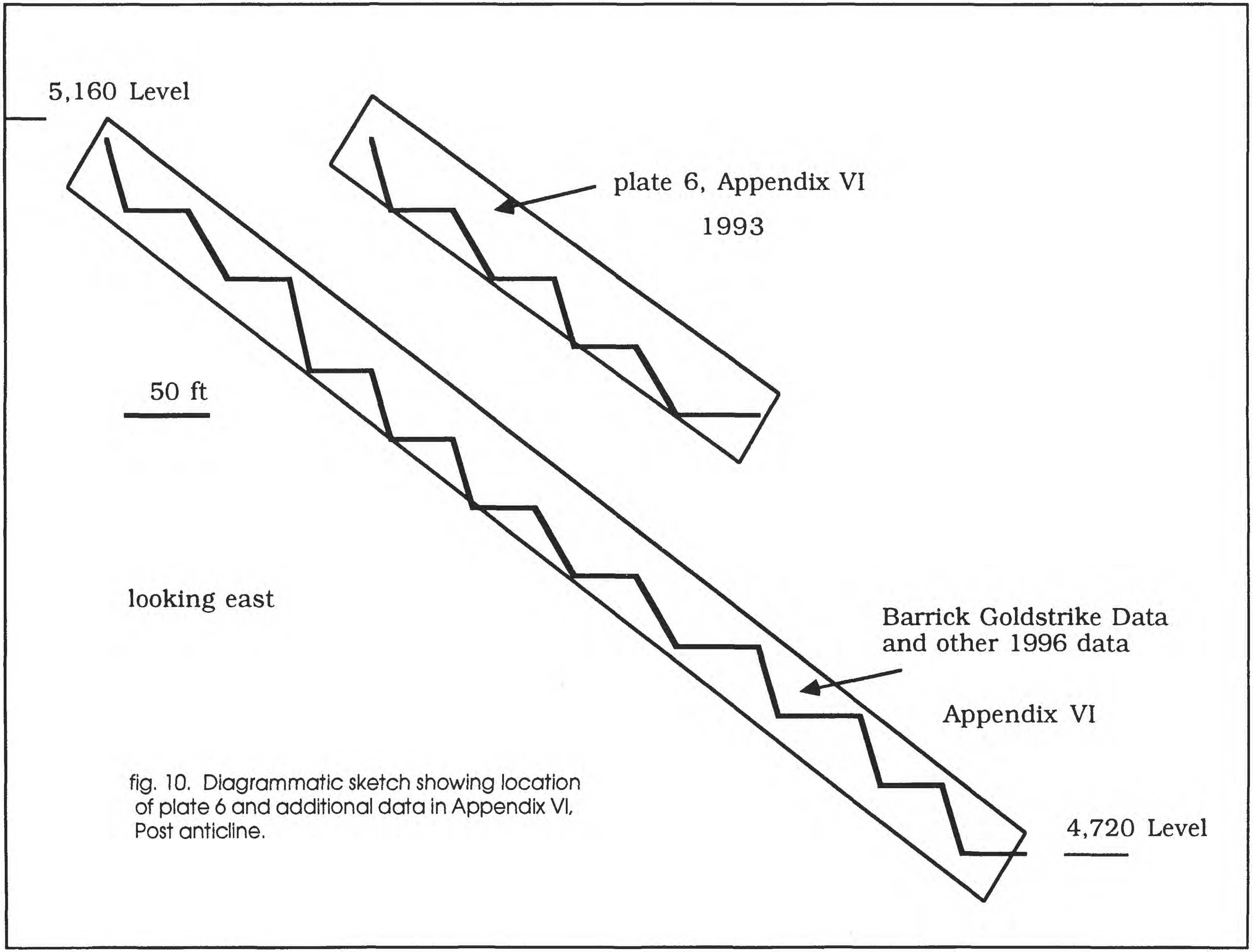

fig. 10. Diagrammatic sketch showing location of plate 6 and additional data in Appendix VI, Post anticline.

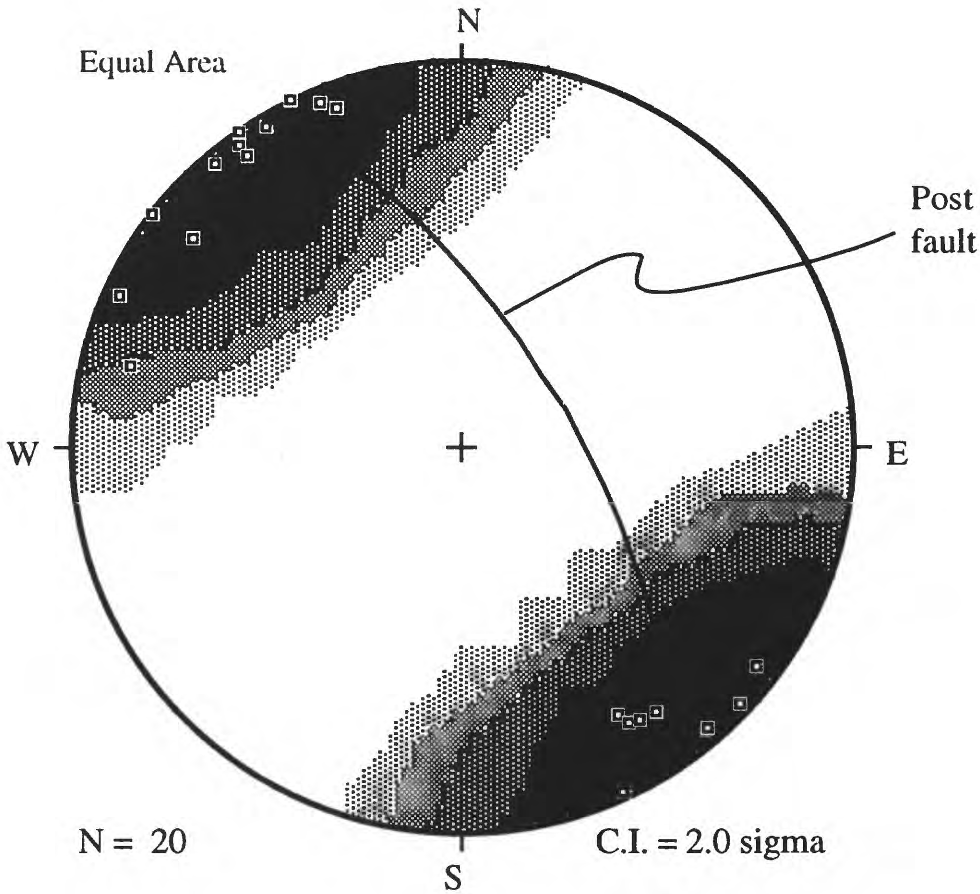

fig. 11. Stereographic net plot showing Kamb contour and scatter plot of fold axes (boxes) in the Post anticline, and approximate Post fault—portrayed as plane—that would lie coplanar with most of the fold axes in the anticline Data from pl.ate 6, from Barrick Goldstrike Mines (BGN) 1″ = 50′ mapping, and additional 1″ = 5′ mapping (SGP); see fig. 10, pl. 6 and Appendix VI. Summary of fold axes as follows (not keyed to boxes):

strike plunge location
1. 215 61 Western gray argillite
2. 149 9 Grand Jean Fault area
3. 294 5 Western argillite
4. 127 6 Western siltstone
5. 150 21 Central black limestone
6. 149 18 Eastern siltstone/argillite
7. 144 16 Eastern limb of anticline
8. 335 17 Total bedding plate 6
10. 139 4 BGM 4720 Level
11. 324 4 BGM 4760 Level
12. 329 4 BGM 4800 Level
13. 334. 0 BGM 4840 Level
14. 325 1 BGM 4880 Level
15. 319 4 BGM 4920 Level
16. 340. 8 BGM 4960 Level
17. 338 5 BGM 5000 Level
18. 133 2 BGM 5040 Level
19. 284 14 BGM 5080 Level
20. 155 1 BGM 5120 Level
21. 324 8 BGM 5160 Level
22. 308 14 SGP 4720 Level, west limb
23. 307 1 SGP 4760 Level, west limb

Conclusions

1. A consistent structural grain is present in the WNW-trending upper central Betze orebody. The *linear fabric* is defined by local WNW-trending fold axes. The *planar fabric* is defined by a WNW-striking, 20° to 30° NE-dipping zone, which contains both the NNE-trending, older fold axes in folds such as the Post anticline, and newer WNW-trending fold and shear zones. The Dillon deformation zone is coplanar with all fold axes in the Goldstrike Mine.

2. The Post fault is coplanar with the plunge of the NW-striking fold axes in the Post anticline.

3. The upper central Betze orebody is hosted in the Dillon deformation zone, which crosscuts the nose of a syncline, parallel to and west of the Post anticline, and generally strikes parallel to the Popovich limestone-granodiorite contact. The orebody is also in the Betze anticline, which may have formed as the result of shear folding along the Dillon deformation zone.

4. The contact between the Popovich limestone and Rodeo Creek unit is deformed in both the upper central Betze orebody, and the Post anticline. Exposures of the contact in the Post anticline are compatible with a depositional contact. However, exposures of phyllonitic rocks and breccia bodies that appear to predate the Dillon deformation zone in the upper central Betze orebody suggest a tectonic contact.

5. At least six separate ore types are defined in the upper central Betze orebody, based on geologic setting, mineralogy, geochemistry, and morphology. The ore types are partitioned spatially within the orebody in discrete oreshoots and have demonstrable spatial relations to the Popovich limestone-Rodeo Creek unit, and Popovich limestone-granodiorite contacts, and the Dillon deformation zone. The gold oreshoots are zoned from the footwall to the hangingwall of the orebody and deformation zone, with pyrite-rich ores on the top, arsenic-rich ores in the central parts, and siliceous, antimony-rich ores at the bottom. The Betze orebody becomes less clay-rich and more siliceous with depth.

Acknowledgments

Funding for field work in 1993 was provided by the Nevada Mining Cooperative and Administered by the Nevada Bureau of Mines and Geology. Field work in 1994 was funded by Barrick Goldstrike Mines, as part of a donation given to the USGS through Chuck Thorman. Access to Barrick

Goldstrike property was facilitated by Keith Bettles, Eric Lauha, and Jeff Volk; Bob Leonardson, Jerry Rahn, and Trevor East, all of Barrick Goldstrike, introduced me to the Betze orebody and provided geologic discussions, assays, and ideas throughout this study. These and other geologists in the mining district have provided fruitful discussion and information. Review of the early manuscript was done by Chuck Thorman and Ted Theodore and resulted in significant improvements.

References cited

Arehart, G.B., Foland, K.A., Naeser, C.W., and Kesler, S.E., 1993, $^{40}Ar/^{39}Ar$, K/Ar, and fission track geochronology of sediment-hosted disseminated gold deposits at Post-Betze, Carlin trend, northeastern Nevada: Economic Geology, v. 88, p. 622–646.

Bettles, K.H., and Lauha, E.A., 1991, Gold deposits of the Carlin Trend, Nevada: World Gold '91, Forum on Technology and Practice, Second Australian Institute of Mining and Metallurgy–Society of mining and Metallurgy Joint Conference, 21-26 April, Cairns, Australia, p. 251–257.

Campbell, B.C., 1994, The geology of the Post oxide deposit, Goldstrike Mine, Eureka County, Nevada: (unpublished) M.S. thesis, Colorado State University, 111 p.

Evans, J.G., and Theodore, T.G., 1978, Deformation of the Roberts Mountains allochthon in north-central Nevada: U.S. Geological Survey Professional Paper 1060, 18 p.

Ketner, K.B., 1987, Post-Early Triassic, pre-middle Eocene folds and thrust faults, northern Adobe Range, Nevada: Geological Society of American Centennial Field-Cordilleran Section, no. 21, p. 91–94.

Ketner K.B., and Alpha, A.G., 1992, Mesozoic and Tertiary rocks near Elko, Nevada—evidence for Jurassic to Eocene folding and low-angle faulting: U.S. Geological Survey Bulletin 1988—C, 13 p.

Ketner, K.B., and Smith, J.F., Jr., 1982, Mid-Paleozoic age of the Roberts thrust unsettled by new data from northern Nevada: Geology, v. 10, p. 298–303.

Ketner, K.B., Murchey, B.L., Stamm, R.G., and Ardlaw, B.R., 1993, Paleozoic and Mesozoic rocks of Mount Icabod and Dorsey Canyon, Elko County, Nevada—evidence for Post-early Triassic emplacement of the Roberts Mountains and Golconda allochthons: U.S. Geological Survey Bulletin 1988—D, 12 p.

Kuehn, C.A., 1989, Studies of disseminated gold deposits near Carlin, Nevada: Evidence for a deep geologic setting of ore formation: unpublished Ph.D. dissertation, Pennsylvania State University, 395 p.

Kuehn, C.A., and Rose, A.W., 1992, Geology and geochemistry of wall rock alteration at the Carlin gold deposit, Nevada: Economic Geology, v. 87,

p. 1697–1721.

Kuehn, C.A., and Rose, A.W., 1995, Carlin gold deposits, Nevada: Origin in a deep zone of mixing between normally pressured and over pressured fluids: Economic Geology, v. 90, p. 17–36.

Lamb, J.B., 1995, A petrographic and fluid inclusion study of the Purple Vein and Post-Betze orebodies, Carlin, Nevada: University of Nevada, Las Vegas, M.S., thesis, 161 p.

Lauha, E.A., and Bettles, K.H., 1993, A geologic comparison of the Post/Betze and Purple vein deposits of the Goldstrike and Meikle Mines, Nevada: Society for Mining, Metallurgy, and Exploration, Preprint 93–170, 20 p.

Leonardson, R.W., and Rahn, J.E., 1996, Geology of the Betze-Post gold deposits, Eureka County, Nevada, *in* Coyner, A.R., and Fahey, eds., Geology and Ore Deposits of the American Cordillera: Geological Society of Nevada, Symposium Proceedings, Reno/Sparks, Nevada, April, 1995, p. 61–94.

Madrid, R.J., 1987, Stratigraphy of the Roberts Mountains allochthon in north-central Nevada: Stanford University, Ph.D. dissertation, 341 p.

Madrid, R.J., and Bagby, W.C., 1986, Structural alignment of sediment-hosted gold deposits in north-central Nevada: An example of inherited fabrics [abs]: Geological Society of America Abstracts with Programs, v. 18, p. 393.

Madrid, R.J.,, R.J., Poole, F.G., and Wrucke, C.T., 1992, Rocks of the Antler orogen—The Roberts Mountain allochthon, *in* Burchfiel, B.C., Lipman, P.W., and Zoback, M.L., eds., The Cordilleran Orogen: Conterminous U.S.: Geological Society of America, The Geology of North America, Volume G–3, p. 28–34.

Oldow, J.S., 1984, Spatial variability in the structure of the Roberts Mountains allochthon, western Nevada: Geological Society of America Bulletin, v. 95, p. 174–185.

Peters, S. G., and Evans J.G, 1995, Mesoscopic and Megascopic fabric geometries in parts of the Carlin trend, Eureka and Elko Counties, Nevada [abs]: *in* Fahey, P ed., Geological Society of Nevada Symposium, Geology and Ore Deposits of the American Cordillera, April 1995., Program with Abstracts, p. 61-62.

Peters, S.G., 1996, Definition of the Carlin trend using orientation of fold axes and applications to ore control and zoning in the central Betze orebody, Betze-Post Mine, *in* Green, Steve ed., Trip B, Structural Geology of the Carlin Trend, Geology and Ore Deposits of the American Cordillera-A Symposium, Field Guide Compendium: Geological Society of Nevada, Reno, Nevada, p. 59-95.

———1997a, Structural transect across the southern Carlin trend, Eureka County, Nevada: U.S. Geological Survey Open-File Report 97—0347, 27 p., 2 sheets, scale 1:500.

———1997b, Structural transect across the central Carlin trend, Eureka County, Nevada: U.S. Geological Survey Open-File Report 97—55, 40 p. 2 sheets, scale 1:6,000.

Radtke, A.S., 1973, Preliminary geologic map of the Carlin Gold Mine, Eureka County, Nevada: U.S. Geological Survey Miscellaneous Field Studies Map MF—537, scale 1:6,000.

———1985, Geology of the Carlin gold deposit, Nevada: U.S. Geological Survey Professional Paper 1267, 124 p.

Roberts, R.J., 1960, Alignment of mining districts in north-central Nevada: U.S. Geological Survey Professional Paper 400—B. p. 17-19.

———1966, Metallogenic provinces and mineral belts in Nevada: Nevada Bureau of Mines Report 13, pt. A, p. 47–72.

Roberts, R.J., Hotz, P.E., Gilluly, J., and Ferguson, H.G., 1958, Paleozoic rocks of north-central Nevada: American Association of Petroleum Geologists Bulletin, v. 42, no. 12, p. 2813–2857.

Sampson, T.R., 1993, Alteration and structural paragenetic relations; with emphasis on Mesozoic imbricate thrust faults, Goldstrike Mines area, Eureka County Nevada: Washington State University, M.S. Thesis, 179 p.

Smith, M.R., and Sharon, R.P., 1994, Engineering geology of Barrick Goldstrike Mines' Betze Pit: Mining Engineering, p. 29–33.

Stewart, J.H., and Carlson, J.E., 1976, Geologic map of north-central Nevada: Nevada Bureau of Mines and Geology, Map 50, scale 1:250,000.

Thorman, C.H., and Christensen, Odin, 1991, Geologic settings of gold deposits in the Great Basin, western United States, *in* Ladeira, E.R., ed., Proceedings of Brazil Gold '91, An international symposium on geology of gold: Belo Horizonte, 1991, A.A. Balkena, Rotterdam, p. 65–76.

Thorman, C.H., Ketner, K.B., Brooks, W.E., Snee, L.W., and Zimmerman, R.A., 1991a, Late Mesozoic-Cenozoic tectonics in northeastern Nevada, *in* Raines, G.I., Lisle, R.W., Schafer, R.W., and Wilkinson, W.H., eds., Geology and Ore Deposits of the Great Basin, Symposium Proceedings: The Geological Society of Nevada, p. 25–45.

Thorman, C.H., Ketner, K.B., Snoke, A.W., Brooks, W.E., and Mueller, K.J., 1991b, Evidence for the involvement of the Roberts Mountains allochthon in Mesozoic tectonics and its effect on mineral deposit and petroleum accumulation models in northeast Nevada, Field Trip 13, *in* Buffa, R.H., and Coyner, A.R., eds., Geology and Ore Deposits of the Great Basin—Field Trip Guidebook Compendium—Great Basin Symposium, April, 1990: Geological Society of Nevada, Reno/Sparks, p. 869–905.

Volk, J.A., and Zimmerman, J.M., 1991, Stratigraphic framework of Ordovician-Devonian rocks at the Goldstrike Mine area, Eureka and Elko Counties, Nevada, The Roberts Mountains Thrust revisited [abs.]: Geological Society of America Abstracts with Programs, v. 23, no. 2, p. 106.

Volk, J.A., Lauha, E., Leonardson, R.W., and Rahn, J.E., 1996, Structural geology of the Betze-Post and Meikle deposits, Elko and Eureka Counties, Nevada Field Trip Guidebook, Trip B - Structural Geology of the Carlin Trend, April 7-9, 1995, Geology and Ore Deposits of the American Cordillera, April 10-13: Geological Society of Nevada, Reno/Sparks, Nevada (in press).

Appendix I.
Bedding attitudes and fold axes from pl. 1, upper central Betze orebody, Goldstrike Mine

N face (pl. 1)
total bedding attitudes

320.0	30.0	N
330.0	45.0	E
345.0	78.0	E
305.0	60.0	N
305.0	30.0	E
290.0	35.0	E
340.0	35.0	N
310.0	42.0	E
312.0	30.0	E
312.0	32.0	E
315.0	8.0	E
325.0	30.0	N
342.0	65.0	N
320.0	5.0	N
255.0	25.0	N
350.0	20.0	N
95.0	20.0	W
348.0	30.0	E
325.0	52.0	E
300.0	32.0	E
20.0	23.0	E
20.0	45.0	E
330.0	50.0	N
180.0	25.0	W
304.0	85.0	N
205.0	55.0	W
155.0	25.0	W
310.0	16.0	E
220.0	16.0	W
135.0	25.0	W
260.0	40.0	N
315.0	42.0	E
50.0	35.0	E

West Face
footwall to Dillon fault zone
bedding attitudes

320.0	30.0	N
330.0	45.0	E
345.0	78.0	E
305.0	60.0	N
305.0	30.0	E
290.0	35.0	E
340.0	35.0	N
310.0	42.0	E
312.0	30.0	E
312.0	32.0	E
315.0	8.0	E
325.0	30.0	N
342.0	65.0	N
320.0	5.0	N
255.0	25.0	N
350.0	20.0	N
95.0	20.0	W
348.0	30.0	E

West Face
Hangingwall to Dillon fault
bedding attitudes

20.0	23.0	E
20.0	45.0	E
330.0	50.0	N
180.0	25.0	W
304.0	85.0	N
205.0	55.0	W
155.0	25.0	W
310.0	16.0	E
220.0	16.0	W
135.0	25.0	W
260.0	40.0	N
315.0	42.0	E
50.0	35.0	E

West Face
fold axes
calculated from stereographic net

1. 331 6 West face, footwall to Dillon fault zone
2. 338 4 West Face, hangingwall to Dillon fault zone
3. 331 5 West Face, total bedding attitudes

Appendix II.

Bedding attitudes and fold axes from pl. 2, upper central Betze orebody, Goldstrike Mine.

1. North Face, Total Footwall (Dillon fault) bedding attitudes

330.0	20.0	N
40.0	85.0	S
110.0	55.0	S
80.0	85.0	S
295.0	45.0	N
250.0	45.0	N
292.0	35.0	N
310.0	40.0	N
278.0	58.0	N
115.0	80.0	S
110.0	90.0	S
305.0	45.0	E
260.0	30.0	N
110.0	12.0	S
250.0	5.0	N
275.0	30.0	N
300.0	25.0	N
275.0	35.0	N

2. North Face Central Rodeo Creek unit Argillite, total bedding attitudes

275.0	40.0	N
245.0	50.0	N
269.0	60.0	N
290.0	25.0	N
252.0	55.0	N
280.0	40.0	N
255.0	40.0	N
277.0	45.0	N
250.0	30.0	N
295.0	17.0	N
195.0	38.0	W
260.0	40.0	N
330.0	25.0	N
310.0	40.0	N
320.0	40.0	N
290.0	42.0	N
190.0	62.0	N
312.0	55.0	E
205.0	45.0	N
340.0	75.0	N
315.0	80.0	E
155.0	78.0	W
188.0	51.0	W
210.0	43.0	N
340.0	50.0	N
254.0	19.0	N
303.0	24.0	N
145.0	50.0	S
280.0	20.0	N
165.0	65.0	W
5.0	68.0	E
273.0	26.0	N
270.0	30.0	N
305.0	30.0	N
295.0	30.0	N
300.0	45.0	N
300.0	60.0	N
300.0	35.0	N

3. North Face Central argillite without folds bedding attitudes

AD

275.0	40.0	N
245.0	50.0	N
269.0	60.0	N
290.0	25.0	N
252.0	55.0	N
280.0	40.0	N
255.0	40.0	N
277.0	45.0	N
250.0	30.0	N
295.0	17.0	N
195.0	38.0	W
260.0	40.0	N
330.0	25.0	N
310.0	40.0	N
320.0	40.0	N
290.0	42.0	N

4. North face Total footwall Dillon fault zone bedding attitudes

330.0	20.0	N
40.0	85.0	S
110.0	55.0	S
80.0	85.0	S
295.0	45.0	N
250.0	45.0	N
292.0	35.0	N
310.0	40.0	N
278.0	58.0	N
115.0	80.0	S
110.0	90.0	S
305.0	45.0	E
260.0	30.0	N
110.0	12.0	S
250.0	5.0	N
275.0	30.0	N
300.0	25.0	N
275.0	35.0	N

5. "CBC" area, north face hangingwall to CBC bedding attitudes

290.0	38.0	N
345.0	45.0	N
310.0	45.0	N
305.0	45.0	N
320.0	25.0	N
320.0	24.0	N
300.0	15.0	N
310.0	35.0	N
289.0	50.0	N
270.0	21.0	N

6. Top (hangingwall) Rodeo Creek unit argillite, bedding attitudes

310.0	25.0	N
295.0	5.0	N
305.0	5.0	N
330.0	25.0	N

7. Soft hangingwall to Dillon fault zone (non argillite rocks) bedding attitudes

280.0	5.0	N
120.0	6.0	S
270.0	10.0	N
270.0	20.0	N
255.0	40.0	N
245.0	40.0	N
240.0	25.0	N
290.0	15.0	N

8. North face (pl. 2) Total bedding attitudes

290.0	38.0	N
345.0	45.0	N
310.0	45.0	N
305.0	45.0	N
320.0	25.0	N
320.0	24.0	N
300.0	15.0	N
310.0	35.0	N
289.0	50.0	N
270.0	21.0	N
275.0	40.0	N
245.0	50.0	N
269.0	60.0	N
290.0	25.0	N
252.0	55.0	N
280.0	40.0	N
255.0	40.0	N
277.0	45.0	N
250.0	30.0	N
295.0	17.0	N
195.0	38.0	W
260.0	40.0	N
330.0	25.0	N
310.0	40.0	N
320.0	40.0	N
290.0	42.0	N
190.0	62.0	N
312.0	55.0	E
205.0	45.0	N
340.0	75.0	N
315.0	80.0	E
155.0	78.0	W
188.0	51.0	W
210.0	43.0	N
340.0	50.0	N
254.0	19.0	N
303.0	24.0	N
145.0	50.0	S
280.0	20.0	N
165.0	65.0	W
5.0	68.0	E

273.0	26.0	N
270.0	30.0	N
305.0	30.0	N
295.0	30.0	N
300.0	45.0	N
300.0	60.0	N
300.0	35.0	N
280.0	5.0	N
120.0	6.0	S
270.0	10.0	N
270.0	20.0	N
255.0	40.0	N
245.0	40.0	N
240.0	25.0	N
290.0	15.0	N
310.0	25.0	N
295.0	5.0	N
305.0	5.0	N
330.0	25.0	N
330.0	20.0	N
40.0	85.0	S
110.0	55.0	S
80.0	85.0	S
295.0	45.0	N
250.0	45.0	N
292.0	35.0	N
310.0	40.0	N
278.0	58.0	N
115.0	80.0	S
110.0	90.0	S
305.0	45.0	E
260.0	30.0	N
110.0	12.0	S
250.0	5.0	N
275.0	30.0	N
300.0	25.0	N
275.0	35.0	N

9. Fold A
Central argillite
Rodeo Creek unit
bedding attitudes

330.0	20.0	N
40.0	85.0	S
110.0	55.0	S
80.0	85.0	S
295.0	45.0	N
250.0	45.0	N

10. Fold B
Central argillite
Rodeo Creek unit
bedding attitudes

190.0	62.0	N
312.0	55.0	E
205.0	45.0	N
340.0	75.0	N
315.0	80.0	E
155.0	78.0	W
188.0	51.0	W
210.0	43.0	N

11. Fold C
Central argillite
Rodeo Creek unit
bedding attitudes

340.0	50.0	N
254.0	19.0	N
303.0	24.0	N

12. Fold D
Central argillite
Rodeo Creek unit
bedding attitudes

145.0	50.0	S
280.0	20.0	N
165.0	65.0	W
5.0	68.0	E
273.0	26.0	N
270.0	30.0	N
305.0	30.0	N
295.0	30.0	N

13. Fold E
Central argillite
Rodeo Creek unit
bedding attitudes

300.0	45.0	N
300.0	60.0	N
300.0	35.0	N

14. Fold F
Central argillite
Rodeo Creek unit
bedding attitudes

292.0	35.0	N
310.0	40.0	N
278.0	58.0	N
115.0	80.0	S
110.0	90.0	S

15. Fold G
Central argillite
Rodeo Creek unit
bedding attitudes

150.0	75.0	W
335.0	35.0	N
320.0	42.0	N
60.0	74.0	E
300.0	10.0	N
265.0	30.0	N

16. Total Fold axes
calculated by stereographic net
North face 1-15

1.	291	4	Footwall rocks, without folds
2.	342	30	Total argillite rocks, w/ folds, Drc
3.	22	34	Central argillite w/o folds, Drc
4.	98	4	Total footwall (Dillon fault) zone
5.	312	4	"CBC" zone, hangingwall area
6.	325	2	Top (hangingwall) argillite, Drc
7.	69	2	Hangingwall to Dillon fault (Dpg, Dpw, Dpb)
8.	329	21	North Face total bedding attitudes
9.	77	14	Fold A central argillite (Drc)
10.	336	37	Fold B central argillite (Drc)
11.	356	19	Fold C central argillite (Drc)
12.	240	18	Fold D central argillite (Drc)
13.	300	0	Fold E central argillite (Drc)
14.	111	3	Fold F central argillite (Drc)
15.	318	1	Fold G central argillite (Drc)

Best fit plane to fold axes is 201/64 ~ Dillon fault zone

Appendix III

Bedding attitudes and fold axes from pl. 3, upper central Betze orebody, Goldstrike Mine.

1. 4800 North face east side folded area bedding attitudes

140.0	80.0	W
320.0	80.0	E
310.0	55.0	E
240.0	10.0	N
325.0	50.0	E
320.0	90.0	E
308.0	56.0	N
330.0	90.0	N
140.0	55.0	S
115.0	58.0	S
295.0	32.0	N
320.0	18.0	N

2. 4800 North face middle area bedding attitudes

180.0	65.0	W
170.0	65.0	W
190.0	50.0	W
295.0	20.0	N
290.0	15.0	N
298.0	18.0	N
250.0	30.0	N
295.0	30.0	N
270.0	20.0	N
309.0	30.0	N
330.0	25.0	N
320.0	42.0	N
318.0	20.0	N
296.0	50.0	E

3. 4840 North face bedding attitudes

284.0	50.0	N
265.0	34.0	N
301.0	42.0	N
300.0	42.0	N
270.0	42.0	N
290.0	40.0	N
230.0	55.0	N
228.0	40.0	N
220.0	20.0	N
300.0	35.0	E
270.0	42.0	N
300.0	35.0	E
320.0	55.0	N
255.0	45.0	N
250.0	20.0	N
250.0	19.0	N
240.0	20.0	N
285.0	32.0	N
300.0	28.0	N
285.0	15.0	N

4. 4880 North face bedding attitudes

285.0	35.0	E
80.0	20.0	E
300.0	25.0	E
280.0	75.0	E
250.0	25.0	N
85.0	40.0	S
95.0	47.0	S
260.0	28.0	N
245.0	15.0	N
255.0	30.0	N
155.0	12.0	W
240.0	45.0	W
250.0	12.0	N
265.0	20.0	N
285.0	30.0	N

5. 4800 Ramp sketch Rodeo Creek unit and Popovich limestone contact figure 5 bedding attitudes

180.0	32.0	N
265.0	30.0	N
*****	.0	N
195.0	25.0	W
150.0	64.0	W
190.0	12.0	W
150.0	64.0	W
260.0	35.0	N
98.0	40.0	S
240.0	32.0	N
310.0	30.0	N
160.0	35.0	W
153.0	52.0	W
260.0	15.0	N
340.0	35.0	N
335.0	65.0	E
340.0	90.0	E
282.0	34.0	N
270.0	25.0	N
288.0	40.0	E
330.0	50.0	E

6. Total bedding attitudes North face, pl. 3

285.0	35.0	E
80.0	20.0	E
300.0	25.0	E
280.0	75.0	E
250.0	25.0	N
85.0	40.0	S
95.0	47.0	S
260.0	28.0	N
245.0	15.0	N
255.0	30.0	N
155.0	12.0	W
240.0	45.0	W
250.0	12.0	N
265.0	20.0	N
285.0	30.0	N
284.0	50.0	N
265.0	34.0	N
301.0	42.0	N
300.0	42.0	N
270.0	42.0	N
290.0	40.0	N
230.0	55.0	N
228.0	40.0	N
220.0	20.0	N
300.0	35.0	E
270.0	42.0	N
300.0	35.0	E
320.0	55.0	N
255.0	45.0	N
250.0	20.0	N
250.0	19.0	N
240.0	20.0	N
285.0	32.0	N
300.0	28.0	N
285.0	15.0	N
180.0	32.0	N
265.0	30.0	N
180.0	.0	N
195.0	25.0	W
150.0	64.0	W
190.0	12.0	W
150.0	64.0	W
260.0	35.0	N
98.0	40.0	S
240.0	32.0	N
310.0	30.0	N
160.0	35.0	W
153.0	52.0	W
260.0	15.0	N
340.0	35.0	N
335.0	65.0	E
340.0	90.0	E
282.0	34.0	N
270.0	25.0	N
288.0	40.0	E
330.0	50.0	E
180.0	65.0	W
170.0	65.0	W
190.0	50.0	W
295.0	20.0	N
290.0	15.0	N
298.0	18.0	N
250.0	30.0	N
295.0	30.0	N
270.0	20.0	N
309.0	30.0	N
330.0	25.0	N
320.0	42.0	N
318.0	20.0	N
296.0	50.0	E
140.0	80.0	W
320.0	80.0	E
310.0	55.0	E
240.0	10.0	N
325.0	50.0	E
320.0	90.0	E
308.0	56.0	N
330.0	90.0	N
140.0	55.0	S
115.0	58.0	S
295.0	32.0	N
320.0	18.0	N

7. Fold axes
calculated by stereographic net
North face, pl. 2

1.	317 3	4800 Level east side, folded area
2.	346 19	4800 Level middle area
3.	346 31	4840 Level
4.	271 3	4880 Level
5.	327 14	4800 Level Ramp sketch, fig. 5
6.	320 16	Total North Face, pl. 3

Appendix IV.
Bedding attitudes and fold axes from pl. 4, upper central Betze orebody, Goldstrike Mine.

1. 4800 North face Limestone (includes parts of pl. 3) bedding attitudes

305.0	35.0	E
310.0	55.0	E
300.0	65.0	E
290.0	35.0	E
290.0	40.0	E
315.0	38.0	E
310.0	50.0	E
305.0	45.0	E
315.0	32.0	E
330.0	45.0	E

2. West Face 4880 bedding attitudes

5.0	35.0	E
358.0	20.0	E
335.0	65.0	E
300.0	25.0	E
300.0	20.0	E
20.0	20.0	E
280.0	40.0	E
300.0	20.0	E
90.0	25.0	S
70.0	10.0	S
350.0	30.0	E
305.0	14.0	E
275.0	25.0	N

3. 4800 West Face bedding attitudes

50.0	25.0	E
.0	30.0	E
310.0	40.0	E
40.0	50.0	E
60.0	35.0	E
300.0	30.0	E
305.0	25.0	E
310.0	40.0	E

4. 4840 West Face bedding attitudes

315.0	58.0	E
312.0	42.0	E
330.0	44.0	E
310.0	32.0	E
295.0	40.0	E
300.0	28.0	E
290.0	35.0	E
300.0	37.0	E
280.0	42.0	E

5. West Face Total (without North Face limestone) bedding attitudes

5.0	35.0	E
358.0	20.0	E
335.0	65.0	E
300.0	25.0	E
300.0	20.0	E
20.0	20.0	E
280.0	40.0	E
300.0	20.0	E
90.0	25.0	S
70.0	10.0	S
350.0	30.0	E
305.0	14.0	E
275.0	25.0	N
300.0	10.0	E
315.0	18.0	E
50.0	25.0	E
.0	30.0	E
310.0	40.0	E
40.0	50.0	E
60.0	35.0	E
300.0	30.0	E
305.0	25.0	E
310.0	40.0	E
315.0	58.0	E
312.0	42.0	E
330.0	44.0	E
310.0	32.0	E
295.0	40.0	E
300.0	28.0	E
290.0	35.0	E
300.0	37.0	E
280.0	42.0	E

6. Fold axes, calculated from stereo net pl. 4 and west part of pl. 5

1.	124	3	4800 Level North Face Limestone
2.	117	9	4880 Level West Face
3.	85	24	4800 Level West Face
4.	356	32	4840 Level West Face
5.	95	18	Total bedding West Face without N Face ls

Appendix V.

Bedding attitudes and fold axes from plate 5, upper central Betze orebody, Goldstrike Mine.

1. East Face, North area bedding attitudes

10.0	50.0	N
285.0	45.0	N
290.0	40.0	N
300.0	45.0	N
310.0	45.0	N
300.0	43.0	N
315.0	55.0	N
300.0	45.0	N
290.0	55.0	N
300.0	55.0	N
320.0	65.0	N
250.0	70.0	N
260.0	55.0	N
290.0	60.0	N
320.0	65.0	N
320.0	40.0	N
185.0	70.0	W
320.0	85.0	N
145.0	40.0	S
335.0	70.0	N
310.0	55.0	N
300.0	45.0	N
310.0	35.0	N
300.0	45.0	N

2. East Face south area bedding attitudes

65.0	15.0	S
240.0	15.0	N
50.0	70.0	S
235.0	75.0	N
2.0	25.0	E
285.0	40.0	N
305.0	30.0	N
60.0	50.0	S
75.0	35.0	S
60.0	50.0	S
70.0	35.0	S
85.0	60.0	S
210.0	70.0	N
200.0	70.0	N

3. East face Total bedding attitudes N and S faces

65.0	15.0	S
240.0	15.0	N
50.0	70.0	S
235.0	75.0	N
2.0	25.0	E
285.0	40.0	N
305.0	30.0	N
60.0	50.0	S
75.0	35.0	S
60.0	50.0	S
70.0	35.0	S
85.0	60.0	S
210.0	70.0	N
200.0	70.0	N
190.0	50.0	N
285.0	45.0	N
290.0	40.0	N
300.0	45.0	N
310.0	45.0	N
300.0	43.0	N
315.0	55.0	N
300.0	45.0	N
290.0	55.0	N
300.0	55.0	N
320.0	65.0	N
250.0	70.0	N
260.0	55.0	N
290.0	60.0	N
320.0	65.0	N
320.0	40.0	N
185.0	70.0	W
320.0	85.0	N
145.0	40.0	S
335.0	70.0	N
310.0	55.0	N
300.0	45.0	N
310.0	35.0	N
300.0	45.0	N

4. Fold axes calculated from stereographic net pl. 5

1.	338	36	North area
2.	56	2	South area
3.	73	34	Total of both areas

Appendix VI.

Bedding attitudes and fold axes from pl. 6, and other areas in the Post Anticline, Goldstrike Mine.

(see figures 2 and 8 for locations) BGM = Barrick Goldstrike Mines data.

1. plate 6
Western gray argillite
bedding attitudes

180.0	6.0	S
85.0	10.0	S
.0	.0	S
80.0	19.0	S
125.0	32.0	S
95.0	22.0	S
89.0	29.0	S
89.0	32.0	S
180.0	25.0	W
120.0	17.0	S
40.0	45.0	E
45.0	54.0	E
128.0	22.0	S

2. plate 6
Grande Jean Fault area
bedding attitudes

30.0	6.0	S
340.0	25.0	E
340.0	10.0	E
335.0	36.0	E
140.0	25.0	W
100.0	15.0	S
80.0	32.0	S
155.0	72.0	W

3. plate 6
Western argillite (Drc)
bedding attitudes

315.0	80.0	N
105.0	52.0	W
115.0	72.0	W
110.0	60.0	W
108.0	80.0	W
220.0	30.0	N
240.0	32.0	N
225.0	35.0	N
95.0	11.0	S
145.0	43.0	W
92.0	34.0	S
80.0	5.0	S
80.0	14.0	S
335.0	50.0	E

4. plate 6
Western siltstone (Dpg)
bedding attitudes

84.0	11.0	S
115.0	25.0	S
140.0	80.0	W
310.0	42.0	N
90.0	44.0	S
90.0	20.0	S
130.0	20.0	W
110.0	20.0	W
140.0	44.0	W
100.0	5.0	W
160.0	70.0	W
135.0	32.0	W
110.0	30.0	W
120.0	25.0	W
120.0	26.0	W
115.0	36.0	S
125.0	42.0	S
120.0	32.0	S
130.0	44.0	S
80.0	20.0	S
98.0	42.0	S
240.0	25.0	W
325.0	35.0	E
250.0	20.0	N
205.0	20.0	N
85.0	32.0	S
60.0	15.0	S
105.0	25.0	S
110.0	47.0	S
110.0	40.0	S
73.0	32.0	S
90.0	40.0	S

5. plate 6
Central black Popovich limestone
bedding attitudes

115.0	50.0	W
105.0	27.0	S
150.0	80.0	W
80.0	36.0	S
87.0	29.0	S
130.0	35.0	S
112.0	33.0	W
140.0	53.0	W
122.0	50.0	W
10.0	40.0	E
128.0	30.0	W
104.0	25.0	S
90.0	26.0	S
112.0	24.0	S
90.0	27.0	S
72.0	28.0	S
90.0	25.0	S
58.0	17.0	S
352.0	45.0	E
345.0	90.0	E
25.0	23.0	S
62.0	39.0	S
80.0	35.0	S
25.0	30.0	S
103.0	25.0	S
135.0	40.0	S
108.0	30.0	W
140.0	75.0	W
108.0	35.0	S
140.0	90.0	S
320.0	70.0	E
324.0	52.0	E
100.0	24.0	S
120.0	24.0	S
82.0	28.0	S
138.0	33.0	W
168.0	36.0	W
90.0	40.0	S
120.0	22.0	S

6. plate 6
Eastern siltstone/argillite
bedding attitudes

150.0	40.0	W
125.0	29.0	W
54.0	40.0	S
175.0	14.0	S
160.0	6.0	S
110.0	15.0	S
340.0	52.0	E
45.0	25.0	E
330.0	55.0	E
39.0	60.0	E
340.0	80.0	E
300.0	90.0	E
325.0	34.0	E
300.0	62.0	E
15.0	60.0	E
155.0	80.0	W
100.0	10.0	W
320.0	80.0	E
140.0	70.0	W
155.0	90.0	W
215.0	90.0	W
305.0	72.0	E
20.0	55.0	E
100.0	10.0	W
25.0	50.0	E
320.0	52.0	E

7. plate 6
Eastern Limb anticline (Drc)
bedding attitudes

90.0	12.0	S
95.0	56.0	S
100.0	11.0	S
80.0	12.0	E
290.0	15.0	N
230.0	39.0	W
95.0	35.0	S
60.0	24.0	E
64.0	20.0	E
40.0	26.0	E
42.0	24.0	E
295.0	90.0	E
78.0	90.0	E
180.0	70.0	S
318.0	30.0	N
304.0	25.0	N
100.0	50.0	S
330.0	39.0	N
336.0	39.0	N
155.0	85.0	W
340.0	62.0	N
110.0	44.0	S
15.0	46.0	E
155.0	34.0	W
155.0	80.0	W
165.0	90.0	W
10.0	50.0	E

8. plate 6

Mudstone (Vinini Formation)
East of Post fault
bedding attitudes

290.0	40.0	N
310.0	53.0	N
323.0	45.0	N
310.0	34.0	N
312.0	39.0	N
315.0	34.0	N
322.0	40.0	N
310.0	30.0	N

9. plate 6
Total bedding attitudes

150.0	40.0	W
125.0	29.0	W
54.0	40.0	S
175.0	14.0	S
160.0	6.0	S
110.0	15.0	S
340.0	52.0	E
45.0	25.0	E
330.0	55.0	E
39.0	60.0	E
340.0	80.0	E
300.0	90.0	E
325.0	34.0	E
300.0	62.0	E
15.0	60.0	E
155.0	80.0	W
100.0	10.0	W
320.0	80.0	E
140.0	70.0	W
155.0	90.0	W
215.0	90.0	W
305.0	72.0	E
20.0	55.0	E
100.0	10.0	W
25.0	50.0	E
320.0	52.0	E
90.0	12.0	S
95.0	56.0	S
100.0	11.0	S
80.0	12.0	E
290.0	15.0	N
230.0	39.0	W
95.0	35.0	S
60.0	24.0	E
64.0	20.0	E
40.0	26.0	E
42.0	24.0	E
295.0	90.0	E
78.0	90.0	E
180.0	70.0	S
318.0	30.0	N
304.0	25.0	N
100.0	50.0	S
330.0	39.0	N
336.0	39.0	N
155.0	85.0	W
340.0	62.0	N
110.0	44.0	S
15.0	46.0	E
155.0	34.0	W
155.0	80.0	W
165.0	90.0	W
10.0	50.0	E

10. plate 6
fold axes
calculated from stereographic net
(see fig. 11)

1.	215	61	Western gray argillite
2.	149	9	Grand Jean Fault area
3.	294	5	Western argillite
4.	127	6	Western siltstone
5.	150	21	Central black limestone
6.	149	18	Eastern siltstone/argillite
7.	144	16	Eastern limb of anticline
8.	335	18	Mudstone (Vinini Formation)
9.	147	17	Total bedding plate 6

Note: the following bedding attitudes are taken from Barrick Goldstrike Mine 1" = 50' scale bench maps from west to east, across the Post anticline at the elevation indicated (see fig. 10).

11. BGM 4720 Level
bedding attitudes

320.0	40.0	N
280.0	15.0	N
340.0	45.0	E
110.0	45.0	S
170.0	30.0	W
200.0	25.0	W
310.0	55.0	E
170.0	85.0	W
340.0	35.0	E
300.0	30.0	E
120.0	30.0	W
110.0	70.0	W
260.0	30.0	W
330.0	60.0	E
320.0	60.0	E
330.0	80.0	E
330.0	70.0	E
320.0	60.0	E
110.0	50.0	S
140.0	55.0	W
100.0	70.0	W
135.0	70.0	W
330.0	80.0	E
320.0	80.0	E
320.0	70.0	E
340.0	60.0	E
325.0	30.0	E
350.0	20.0	E

12. BGM 4760 Level
bedding attitudes

300.0	50.0	E
320.0	10.0	E
290.0	40.0	E
310.0	25.0	E
310.0	30.0	E
5.0	35.0	E
330.0	75.0	E
350.0	55.0	E
350.0	55.0	E
310.0	30.0	N
220.0	30.0	N
230.0	15.0	N
130.0	30.0	S
320.0	35.0	E
30.0	35.0	E
330.0	20.0	E
340.0	55.0	E
320.0	25.0	E
290.0	30.0	N
310.0	40.0	E
310.0	30.0	E
300.0	20.0	E
330.0	25.0	E
100.0	5.0	S
355.0	30.0	E
260.0	20.0	N
190.0	30.0	W
150.0	70.0	W
140.0	50.0	W
120.0	55.0	W
250.0	15.0	N
290.0	45.0	N
300.0	50.0	N
270.0	40.0	N
250.0	20.0	N
250.0	10.0	N
300.0	30.0	N
290.0	55.0	N
330.0	45.0	E
325.0	70.0	E
335.0	65.0	E
325.0	75.0	N
320.0	70.0	N
290.0	80.0	N
305.0	30.0	N
80.0	40.0	S
350.0	65.0	E
20.0	45.0	E

13. BGM 4800 Level
bedding attitudes

310.0	30.0	E
310.0	30.0	E
250.0	10.0	N
130.0	40.0	W
200.0	25.0	W

330.0	65.0	E
340.0	60.0	E
290.0	20.0	N
170.0	80.0	W
320.0	75.0	E
340.0	75.0	E
330.0	40.0	E
290.0	45.0	N
340.0	55.0	E
290.0	30.0	E
350.0	60.0	E
190.0	20.0	W
330.0	50.0	E
250.0	15.0	N
320.0	50.0	E
330.0	15.0	E
320.0	60.0	E
110.0	30.0	S
100.0	30.0	S
175.0	35.0	W
150.0	20.0	W
130.0	20.0	W
195.0	22.0	W
220.0	15.0	W
300.0	15.0	N
330.0	40.0	E
330.0	40.0	E
320.0	35.0	E
315.0	40.0	E
100.0	40.0	S
310.0	40.0	E
340.0	35.0	E
355.0	25.0	E
320.0	70.0	E

14. BGM 4840 Level bedding attitudes

300.0	20.0	E
310.0	.0	E
250.0	30.0	N
10.0	50.0	E
320.0	60.0	E
220.0	30.0	N
170.0	40.0	W
230.0	15.0	N
265.0	35.0	N
240.0	35.0	N
320.0	35.0	E
320.0	35.0	E
110.0	20.0	S
340.0	20.0	E
10.0	30.0	E
190.0	20.0	W
20.0	30.0	E
50.0	35.0	S
350.0	25.0	E
330.0	60.0	E
130.0	35.0	W
125.0	40.0	W
320.0	65.0	E
350.0	60.0	E
10.0	45.0	E
220.0	15.0	N
170.0	20.0	W
100.0	45.0	S
110.0	25.0	S

15. BGM 4880 Level bedding attitudes

150.0	15.0	W
150.0	20.0	W
250.0	25.0	N
300.0	20.0	E
120.0	25.0	W
240.0	15.0	N
160.0	10.0	W
280.0	30.0	N
330.0	25.0	E
280.0	35.0	E
30.0	20.0	S
140.0	35.0	W
20.0	30.0	E
110.0	20.0	S
140.0	30.0	W
150.0	30.0	W
150.0	35.0	W
220.0	30.0	W
300.0	45.0	N
320.0	50.0	E
140.0	20.0	W
160.0	20.0	W
40.0	30.0	E
170.0	6.0	W
140.0	25.0	W
160.0	20.0	W
170.0	15.0	W
330.0	20.0	E
40.0	10.0	E
310.0	40.0	N
340.0	87.0	N
330.0	25.0	E
15.0	40.0	E
320.0	20.0	E

16. BGM 4920 Level bedding attitudes

255.0	15.0	W
160.0	15.0	W
130.0	25.0	S
305.0	45.0	N
350.0	25.0	E
240.0	15.0	N
140.0	20.0	W
260.0	15.0	N
310.0	10.0	E
320.0	50.0	E
140.0	20.0	W
160.0	20.0	W
340.0	15.0	E
170.0	15.0	W

17. BGM 4960 Level bedding attitudes

170.0	20.0	W
160.0	30.0	W
300.0	25.0	E
140.0	25.0	S
220.0	30.0	N
190.0	25.0	W
150.0	25.0	W
310.0	15.0	E
220.0	15.0	W
230.0	15.0	N
240.0	20.0	N
300.0	25.0	N
165.0	35.0	W
175.0	25.0	W
340.0	80.0	E
310.0	30.0	N
355.0	50.0	E
170.0	15.0	W
330.0	35.0	N
160.0	80.0	W
340.0	15.0	E
340.0	20.0	E
340.0	60.0	E

18. BGM 5000 Level bedding attitudes

210.0	25.0	W
95.0	25.0	S
140.0	35.0	W
115.0	20.0	S
240.0	10.0	N
280.0	30.0	N
280.0	45.0	N
200.0	18.0	W
320.0	30.0	N
210.0	35.0	W
150.0	15.0	W
160.0	10.0	W
178.0	10.0	W
140.0	20.0	W
30.0	15.0	E
220.0	30.0	W
177.0	30.0	W
300.0	25.0	N
330.0	15.0	E
350.0	40.0	E
350.0	40.0	E
350.0	45.0	E

19. BGM 5040 Level bedding attitudes

250.0	20.0	N
175.0	25.0	W
165.0	30.0	W
140.0	55.0	W
140.0	35.0	W
95.0	40.0	W
310.0	25.0	E
330.0	35.0	N
265.0	20.0	N
100.0	35.0	S
320.0	20.0	N
125.0	20.0	W
170.0	20.0	W
55.0	45.0	E
340.0	25.0	E
125.0	20.0	S
50.0	15.0	E

20. BGM 5080 Level bedding attitudes

170.0	40.0	W
230.0	30.0	N
200.0	35.0	W
320.0	20.0	N
300.0	12.0	N
130.0	30.0	W
100.0	32.0	S
100.0	50.0	S
140.0	40.0	W

21. BGM 5120 Level bedding attitudes

130.0	10.0	W
140.0	25.0	W
170.0	15.0	W
350.0	45.0	N
150.0	20.0	W
160.0	25.0	W
130.0	25.0	S
200.0	10.0	W
200.0	10.0	W
330.0	15.0	E
150.0	75.0	W

22. BGM 5160 Level bedding attitudes

250.0	20.0	N	340.0	10.0	E
155.0	25.0	W	300.0	35.0	E
160.0	35.0	W	150.0	50.0	W
165.0	40.0	W	140.0	.0	W

Note: The following bedding attitudes were taken at the indicated elevations on the accessible western limb of the Post anticline, and are the same exposures measured by the data marked BGM above.

23. SGP 4720 Level bedding attitudes

150.0	20.0	W
218.0	28.0	W
115.0	30.0	S
138.0	45.0	W
195.0	34.0	W
290.0	34.0	N
315.0	30.0	N
264.0	70.0	N
330.0	32.0	N
315.0	55.0	N
315.0	34.0	N
310.0	60.0	N
250.0	35.0	N
275.0	38.0	N
275.0	35.0	N
305.0	25.0	N
270.0	40.0	N
270.0	35.0	N

24. SGP 4760 Level bedding attitudes

145.0	65.0	W
140.0	35.0	W
286.0	35.0	N
40.0	65.0	S
125.0	68.0	S
80.0	47.0	S
105.0	30.0	S
110.0	50.0	S
120.0	65.0	W
120.0	90.0	W
295.0	7.0	N
205.0	42.0	N
307.0	50.0	N
270.0	45.0	N
53.0	20.0	S
310.0	42.0	N
270.0	54.0	N
310.0	30.0	N
105.0	28.0	S
165.0	68.0	W
330.0	40.0	N
315.0	46.0	N
10.0	26.0	S
125.0	71.0	W
125.0	46.0	W
115.0	90.0	W
165.0	90.0	W
135.0	45.0	W
175.0	55.0	W
255.0	48.0	W
350.0	20.0	N
240.0	50.0	N
240.0	35.0	N
105.0	30.0	W
260.0	20.0	N
345.0	20.0	N
330.0	52.0	N
328.0	20.0	N
320.0	35.0	N
320.0	50.0	N
305.0	60.0	N

25. Post anticline fold axes, calculated by stereographic net from BGM and other data (see fig. 11).

11.	139.0	4.0	BGM 4720 Level
12.	324.0	4.0	BGM 4760 Level
13.	329.0	4.0	BGM 4800 Level
14.	334.0	.0	BGM 4840 Level
15.	325.0	1.0	BGM 4880 Level
16.	319.0	4.0	BGM 4920 Level
17.	340.0	8.0	BGM 4960 Level
18.	338.0	5.0	BGM 5000 Level
19.	133.0	2.0	BGM 5040 Level
20.	284.0	14.0	BGM 5080 Level
21.	155.0	1.0	BGM 5120 Level
22.	324.0	8.0	BGM 5160 Level
23.	308.0	14.0	SGP 4720 Level, west limb
24.	307.0	1.0	SGP 4760 Level, west limb